City Research Online

City St George's, University of London

Citation: Roberts, P. A., Thomas, C. N., Plaice, G. B., Roberts, J. A., Jones, M-C., Andrews, J. W. & Hill, L. J. (2025). Mathematical models of topically and intravitreally applied ranibizumab. Investigative Ophthalmology and Visual Science, 66(11), 45. doi: 10.1167/iovs.66.11.45

This is the published version of the paper.

This version of the publication may differ from the final published version. To cite this item please consult the publisher's version.

Permanent repository link: https://openaccess.city.ac.uk/id/eprint/35415/

Link to published version: https://doi.org/10.1167/iovs.66.11.45

Copyright and Reuse: Copyright and Moral Rights remain with the author(s) and/or copyright holders. Copies of full items can be used for personal research or study, educational, or not-for-profit purposes without prior permission or charge, unless otherwise indicated, provided that the authors, title and full bibliographic details are credited, a hyperlink and/or URL is given for the original metadata page and the content is not changed in any way. For full details of reuse please refer to City Research Online policy.

City Research Online: http://openaccess.city.ac.uk/ publications@citystgeorges.ac.uk

Mathematical Models of Topically and Intravitreally Applied Ranibizumab

Paul A. Roberts[1,2] Chloe N. Thomas[3] Gabriel Bellamy Plaice[3] James A. Roberts[3] Marie-Christine Jones[4] James W. Andrews[5] and Lisa J. Hill[3,6]

[1]Centre for Systems Modelling and Quantitative Biomedicine, University of Birmingham, Birmingham, United Kingdom
[2]Department of Optometry and Visual Sciences, City St George's, University of London, London, United Kingdom
[3]Department of Biomedical Sciences, University of Birmingham, Birmingham, United Kingdom
[4]School of Pharmacy, University of Birmingham, Birmingham, United Kingdom
[5]School of Mathematics, University of Birmingham, Birmingham, United Kingdom
[6]Birmingham Biomedical Research Centre, National Institute for Health and Care Research, University Hospitals Birmingham, Birmingham, United Kingdom

Correspondence: Paul A. Roberts, Department of Optometry and Visual Sciences, City St George's, University of London, London EC1V 0HB, UK; p.a.roberts@univ.oxon.org.

Received: December 21, 2024
Accepted: June 29, 2025
Published: August 20, 2025

Citation: Roberts PA, Thomas CN, Bellamy Plaice G, et al. mathematical models of topically and intravitreally applied ranibizumab. *Invest Ophthalmol Vis Sci.* 2025;66(11):45. https://doi.org/10.1167/iovs.66.11.45

Purpose. Wet age-related macular degeneration (AMD) causes vision loss when vascular endothelial growth factor (VEGF) stimulates blood vessel growth into the light-sensitive retina. Anti-VEGF treatments such as ranibizumab are currently administered to treat wet AMD via intravitreal injections, which are unpleasant, expensive, and risk complications. We explored the efficacy of topically administered ranibizumab, with cell-penetrating peptides (CPPs).

Methods. Ex vivo pig eyes were divided into three groups and treated with (1) topical or (2) intravitreal ranibizumab and CPP, or (3) intravitreal ranibizumab. ELISAs measured ranibizumab and VEGF concentrations in the aqueous and vitreous at 20 min, 40 min, 1 h, and 3.5 h ($n = 3$, per group). An ordinary differential equation model was formulated to describe the evolving concentrations of ranibizumab, VEGF, and their compounds in the tear, aqueous, and vitreal compartments.

Results. Experimental—Topical: aqueous ranibizumab levels increased significantly, coincident with a significant drop in aqueous VEGF. Vitreal ranibizumab increased significantly, while vitreal VEGF remained constant. Intravitreal (with and without CPP): vitreal ranibizumab reached high concentrations, coincident with a significant drop in vitreal VEGF. Mathematical—topical treatment may provide sustained, moderate suppression of vitreal VEGF levels, while intravitreal treatment provides strong suppression, which lessens between treatments.

Conclusions. CPP allows topical ranibizumab to penetrate the cornea. Combined intravitreal/topical treatment presents a promising approach; topical treatment suppresses vitreal VEGF levels between injections and thereby potentially reduces the frequency of injections. Treatment efficacy would be enhanced if ranibizumab's rate of binding to VEGF or tear residence time could be increased.

Keywords: age-related macular degeneration, ranibizumab, cell-penetrating peptides, pharmacokinetics, pharmacodynamics

Intravitreal injections, the standard mode of drug administration for wet age-related macular degeneration (AMD), are unpleasant, expensive, and risk complications. In this article, we take a combined experimental-modeling approach, exploring the potential for topical administration to replace or augment intravitreal treatment.

AMD is a degenerative retinal disease, which leads to irreversible loss of central vision. Affecting approximately 196 million people worldwide, it is a growing health and economic burden, with 288 million cases expected by 2040.[1] AMD progresses through early, intermediate, and late stages.[2] The late stage comes in two forms: dry and wet.[2] Dry AMD involves the degeneration of the neural retina, retinal pigment epithelium, and choroid in a process known as geographic atrophy, while wet AMD is marked by choroidal neovascularization (CNV), wherein, encouraged by vascular endothelial growth factor (VEGF), blood vessels from the choroidal vasculature undergo aberrant growth, penetrating and damaging the retina.[3–5]

Wet AMD is currently treated with regular, invasive, intravitreal injections of anti-VEGF biological drugs, such as ranibizumab, bevacizumab, and aflibercept,[6] which bind to and neutralize VEGF,[6] reducing CNV and slowing vision loss. These injections are expensive, due, in part, to the need for regular medical appointments, and are associated with complications, including discomfort, endophthalmitis, retinal detachments, and subconjunctival hemorrhages, resulting in suboptimal drug adherence from patients.[7] As such,

Copyright 2025 The Authors

This work is licensed under a Creative Commons Attribution 4.0 International License.

Downloaded from iovs.arvojournals.org on 09/24/2025

there is an urgent clinical need to develop less invasive drug-delivery approaches.[8]

Topical delivery provides a promising, noninvasive alternative, in the form of eye drops or drug-eluting contact lenses (which are in development but not currently in clinical use for anti-VEGF treatments).[9,10] While promising, these delivery methods present new challenges, including the difficulty of transporting anti-VEGF molecules across the cornea (mostly because current anti-VEGF molecules are all fairly large), and the need to achieve therapeutic doses at the back of the eye, overcoming various barriers (e.g., aqueous-vitreous and vitreo-retinal interfaces) and clearance mechanisms (e.g., tear and aqueous clearance and dilution).[11] The first of these challenges may be overcome using cell-penetrating peptides (CPPs), positively charged short peptide chains that serve as chaperones for therapeutics, enhancing their delivery through tissues.[12,13] Preclinical studies have demonstrated that CPPs may aid drug delivery to the retina,[14] including the delivery of ranibizumab and bevacizumab[9] (and to other structures with notoriously obstructive barriers such as the skin[15] and cell plasma membranes[16]).

In this study, we explore the potential of topically delivered ranibizumab and a polyarginine based CPP for the treatment of wet AMD, taking both experimental and mathematical approaches. Experimentally, we use an ex vivo porcine model to measure ranibizumab and VEGF concentrations over time, in the aqueous and vitreous, following topical or intravitreal administration (extending de Cogan et al.,[9] which considered only a single time point in porcine eyes and did not measure aqueous or VEGF concentrations). Mathematically, we develop an ordinary differential equation (ODE) model to describe and predict the evolving concentrations of ranibizumab, VEGF, and their compounds in the tear, aqueous, and vitreous. Our model is based on that of Hutton-Smith et al.,[17] with a number of important differences; most significantly, we include a tear compartment and a modified aqueous-vitreous exchange term to allow for the passage of ranibizumab, VEGF, and their compounds in both directions across the aqueous-vitreous interface (where before they could move only in the vitreous to aqueous direction). Fitting this model to our experimental data, we use it to extrapolate to the in vivo human eye, predicting treatment efficacy for a range of treatment regimens and scenarios. Previous modeling studies have explored both compartmental ODE[17–20] and spatially resolved partial differential equation models[21–26] for ocular drug delivery, spanning a variety of drugs, modes of administration, and diseases. See reviews of mathematical models of ocular drug delivery[27–30] and of the retina[31] for a detailed overview of previous modeling work in this area.

Methods

Experimental Methods

CPP Formulation. Lyophilized CPPs, ~6 amino acids long, were purchased from Genscript, Oxford, UK (SC1208) and reconstituted in sterile, nuclease-free water.

Ranibizumab Formulation. A total of 1 mg of humanized anti-VEGF monoclonal antibody fragments (ranibizumab) was purchased already constituted in PBS from MedChem Express (CAT: HY-P9951A-1mg; Princeton, NJ, USA) and stored at −80°C.

Zeta Potential. It is thought that CPP molecules may need to bind to ranibizumab molecules in order to facilitate their transport across the cornea.[32] The extent of complexation will depend upon the ratio of CPP to ranibizumab molecules present. We determined the appropriate ratio by measuring the zeta potential of preparations containing a range of CPP/ranibizumab concentration ratios. This provided a distribution of measured effective charges from which we could assess if sufficient complexation had occurred.

Ranibizumab (1 mg mL^{-1}) and CPP (20–100 mg mL^{-1}) solutions were prepared in water. Complexes were produced by mixing the antibody and CPP at various concentration (ranibizumab/CPP—1:1, 1:10, 1:20, 1:25, 1:50, 1:100, 10:10, 10:25, and 10:50) and volume (ranibizumab vol./CPP vol.—1:1, starting with 10 or 50 µL ranibizumab, and 1:2, 1:3, and 1:5, starting with 10 µL ranibizumab) ratios in a 96-well plate at room temperature. The zeta potential of the complexes was assessed by electrophoretic light scattering on a Nanosizer ZS (Malvern Panalytical, Malvern, Worcestershire, UK) after dilution in aqueous sodium chloride to adjust conductivity (10 µL of complexes with NaClaq 5–7 mM). All measurements were performed at room temperature.

For most complexes, bi- or trimodal distributions were observed. When CPP concentration was low (<50 mg mL^{-1}), results were more variable, potentially due to low complex concentration and, therefore, increased noise. As the CPP concentration was increased to 50 or 100 mg mL^{-1}, measurements appeared more robust, with improved quality. For the 1:100 mg mL^{-1} complexes, average zeta potential values were slightly positive (ca. 4–6 mV), with the presence of strongly positive complexes (>15 mV) noted within some of the samples. The change in zeta potential observed following CPP addition suggests successful formation of the complexes.

A concentration ratio of 1:100 mg mL^{-1} was selected for the preparation of the complexes for the ex vivo experiments, which corresponds to a large molar excess of CPPs compared to the monoclonal antibody fragment. The zeta potential of the complexes was measured 24 hours after preparation. Zeta potential appeared stable within this time frame, with values ca. 3 to 6 mV. Two populations were detected with zeta potentials ca. ±15 mV.

Administering Treatment to Ex Vivo Porcine Eyes. A total of 39 fresh, unscalded ex vivo porcine eyes were delivered in a cooled box <24 h after death (all experiments and procedures involving animals adhered to the ARVO Statement for the Use of Animals in Ophthalmic and Vision Research). On arrival, the eyes were placed in phosphate-buffered saline after removing excess tissue. Eye diameters (length and height/width) were recorded using a calliper to inform geometrical parameters in the mathematical model. Eyes were placed in 6-well plates, supported with foam inserts, and 45 µL of therapeutics was applied either as a topical drop or via intravitreal injection.

The experimental groups are listed in Table 1 (with 12 eyes for each of the three treatment groups and 3 eyes

Table 1. Experimental Treatment Groups

Treatment	Delivery Method	Eyes (*n*)
Ranibizumab* and CPP†	Topical drop	12
Ranibizumab* and CPP†	Intravitreal injection	12
Ranibizumab*	Intravitreal injection	12
Sterile water	Intravitreal injection	3

* Ranibizumab doses were all 1 mg mL^{-1}.
† CPP doses were all 100 mg mL^{-1}.

Investigative Ophthalmology & Visual Science

Downloaded from iovs.arvojournals.org on 09/24/2025

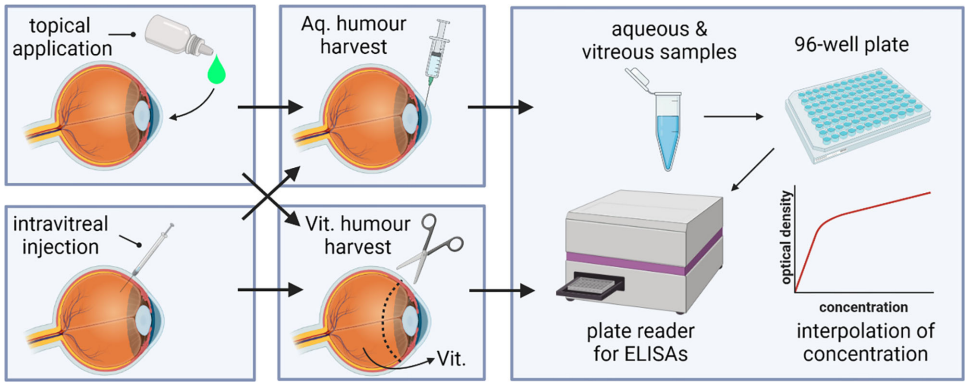

Figure 1. Diagram of the experimental procedure. Porcine eyes were treated either topically or via intravitreal injection. The aqueous humor was collected using a syringe, while the vitreous humor was harvested after removal of the anterior segment. Ranibizumab and VEGF levels were detected using ELISA, and the optical density of the fluids was measured using a plate reader and then converted into a concentration using the respective standard curves. Figure created in https://BioRender.com/g17g888.

for controls). Eyes received either a topical eye drop of ranibizumab (1 mg mL^{-1}) and CPP (100 mg mL^{-1}), an intravitreal injection of ranibizumab (1 mg mL^{-1}) and CPP (100 mg mL^{-1}), or an intravitreal injection of ranibizumab alone (1 mg mL^{-1}). The remaining three eyes received an intravitreal injection of sterile water as a control (see Fig. 1). Eyes were then placed on a shaker at room temperature, approximating the saccadic/translational motion to which living eyes would be subject, and promoting mixing in both aqueous and vitreal compartments, consistent with our mathematical modeling assumption (see the Model Formulation section below; all eyes were shaken under the same conditions for the relevant time frames, e.g., for the preceding 20 min where measurements were made at 20 min, and for the preceding 40 min, where measurements were made at 40 min, etc.). At times 20 min, 40 min, 1 h, and 3.5 h, the aqueous and vitreous humor were extracted and processed to determine VEGF and ranibizumab concentrations (with $n = 3$ eyes per time point, per group).

Sample Collection. Aqueous was extracted by making an incision in the cornea and using a Hamilton syringe to extract 200 µL of aqueous humor, which was stored in Eppendorfs on ice. To collect the vitreous, the cornea was surgically removed at the limbus and the vitreous dissected using tweezers, collected in a Falcon tube, and homogenized. The homogenized vitreous was then centrifuged and the supernatant collected and stored at 4°C (see Fig. 1).

ELISA. The aqueous and vitreous samples were analyzed by ELISA to detect levels of either VEGF-A (Invitrogen, Paisley, UK; Cat: #ES25RB) or ranibizumab (Abcam, Cambridge, UK; Cat: #ab282900). Both kits were performed according to the manufacturer's instructions. Samples were diluted twofold in Assay Buffer. Standards, controls, and samples (100 µL) were added to wells and incubated at room temperature for 30 min. After incubation, the plate was washed three times with wash buffer, and then the horseradish peroxidase–conjugate probe was added and incubated again. The incubation solution was discarded, and the wells were washed before adding 3,3′,5,5′-tetramethylbenzidine (TMB) substrate, followed by a 10-min dark incubation. Stop solution was added, changing the color from blue to yellow. A standard curve was prepared as per the manufacturer's instructions, excluding standard zero. Optical density values were plotted against ranibizumab concentrations, and sample concentrations were obtained by multiplying by the dilution factor (see Fig. 1).

Statistical Analysis of ELISA Data. A two-sample Kolmogorov–Smirnov test was used to determine the statistical significance of changes in ranibizumab and VEGF levels following topical or intravitreal treatment in our ex vivo porcine experiments (see the Experimental Results section), judging P values below 0.05 to be statistically significant. The two-sample Kolmogorov–Smirnov test is a nonparametric test that can be used to determine the likelihood that two sets of samples come from the same probability distribution. We employed the MATLAB (R2020a) routine kstest2 with default settings.

Model Formulation

We construct a mathematical model to predict the evolving concentrations of VEGF, ranibizumab, and their compounds as they transition between compartments and interact within the human or porcine eye. The model takes the form of a set of ODEs, which describe the rate at which these concentrations change over time.

For simplicity, we do not model CPPs explicitly. Whether they operate by binding to ranibizumab or act directly on the cornea, the end result is to increase corneal permeability to ranibizumab, which is accounted for through an appropriate choice of the corneal permeability coefficient, $\beta_{\text{Tear-Aq},r}$ (cm h^{-1}; see Equations 3 and 5 below). In the case that CPPs do bind to ranibizumab, we assume that this has a negligible effect on its interaction with VEGF.

Biochemically, VEGF (V) can bind to either one or two molecules of ranibizumab (R), forming VEGF-ranibizumab (VR) and ranibizumab-VEGF-ranibizumab (RVR), respectively.[33] The reaction kinetics are as follows:

$$\mathrm{V} + \mathrm{R} \underset{k^-}{\overset{2k^+}{\rightleftharpoons}} \mathrm{VR}, \tag{1a}$$

$$\mathrm{R} + \mathrm{VR} \underset{2k^-}{\overset{k^+}{\rightleftharpoons}} \mathrm{RVR}, \tag{1b}$$

where k^+ (pmol^{-1} mL h^{-1}) is the binding rate of R to VR, and k^- (h^{-1}) is the unbinding rate of VR. We assume, with Hutton-Smith et al.,[17] that the rate of binding(/unbinding) of R to(/from) each site on V is the same, regardless of whether the other site is filled. Since there are two empty binding sites available on V, the binding rate of R to V is $2k^+$, twice

Investigative Ophthalmology & Visual Science

Downloaded from iovs.arvojournals.org on 09/24/2025

Table 2. Independent and Dependent Variables Used in the Mathematical Models (See Equations 2–13)

Variable	Description (Units)
t	Time (h)
V_{Tear}	Tear volume (mL)
v_i	VEGF (V) concentration ($i \in$ {Aq, Vit}) (pmol mL^{-1})
r_i	Ranibizumab (R) concentration ($i \in$ {Tear, Aq, Vit}) (pmol mL^{-1})
u_i	VEGF-ranibizumab (VR) concentration ($i \in$ {Aq, Vit}) (pmol mL^{-1})
w_i	Ranibizumab-VEGF-ranibizumab (RVR) concentration ($i \in$ {Aq, Vit}) (pmol mL^{-1})

Time, t, is the independent variable: a given for the models. The remaining variables are dependent variables: the quantities for which we are solving our models.

that of R to VR, where only one binding site is available. Similarly, the unbinding rate of RVR is $2k^-$, since either of the Rs can unbind to form R + VR.

The model is divided into three physical compartments: the tear film (the fluid layer covering the anterior surface of the cornea; this compartment is only modeled when considering topical treatments), the aqueous humor (filling the anterior segment), and the vitreous humor (filling the posterior segment). We describe the evolving concentrations of V, R, VR, and RVR in the aqueous (Aq) and vitreal (Vit) compartments, and of R in the tear film (Tear) compartment, together with the variation in volume of the tear film with application and drainage of eye drops. See Table 2 for a full list of model variables and Figure 2 for a model diagram and schematic.

In choosing an ODE model, we are making the assumption that the chemical species modeled in each physical compartment are well-mixed. This is a justified simplification given the low volume of the tear film and aqueous, as well as the mixing effect of the fluid flow within them, and given the mixing effect of saccadic eye rotations within the vitreous, especially in the partially liquefied aged vitreous of patients with AMD.[21–23,25,26]

In what follows, we define the model in its most general form, which applies to an in vivo human eye with topical application of ranibizumab. We then describe how the equations are simplified for intravitreal injections and/or for an ex vivo porcine eye. Two subcases of the topical treatment case are considered: *drop-based therapy* (as in our experiments; see Experimental Methods section) and *drug-eluting contact lenses*.[10] For topical drops, tear volume and ranibizumab concentration deplete following drop application, while for drug-eluting contact lenses, tear volume and ranibizumab concentration are assumed to remain constant while a lens is worn. (When fitting to ex vivo porcine experimental data, we also consider the scenario where the tear ranibizumab concentration depletes, but the tear/applied drop volume is held constant.)

The MATLAB (R2020a) routine ode45, which employs an explicit Runge–Kutta method, was used for solving all versions of our ODE model.

Tear Film (Tear) Compartment. This compartment is used only when considering topical treatments. When using a drug-eluting contact lens, the tear film volume, $V_{\text{Tear}}(t)$ (mL), remains fixed at its normal volume, $V_{\text{Tear}_{\text{Norm}}} = 6.35 \times 10^{-3}$ mL, whereas, when treating with eye drops, V_{Tear} is a function of time, t (h), since the last drop was applied. The eye drops in our study have a volume of $V_{\text{Drop}} = 4.5 \times 10^{-2}$ mL, while the maximum volume of fluid that can be held in the tear film, known as the reservoir

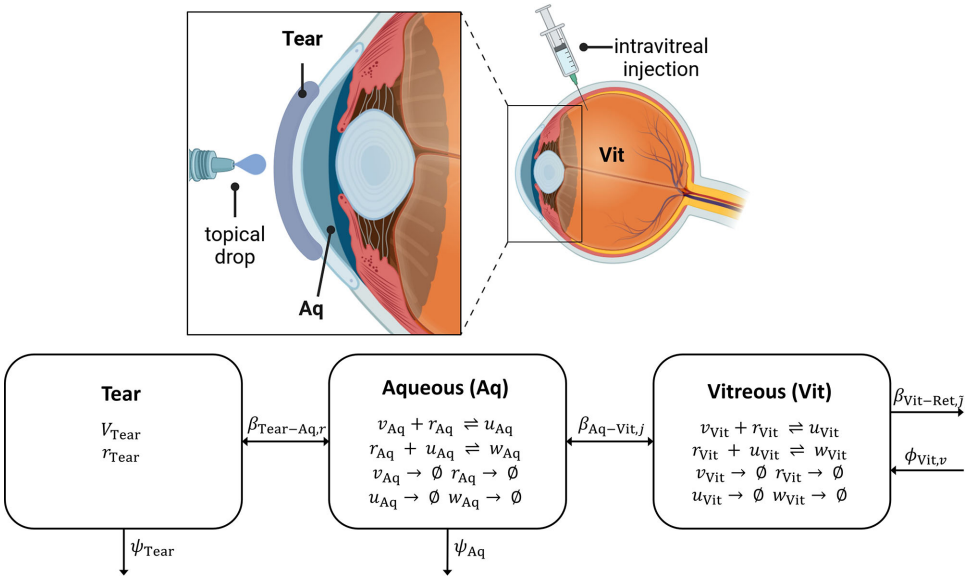

Figure 2. Anatomical and schematic diagrams for the mathematical model. *Top*: anatomical diagram, showing the locations of the tear film (Tear), aqueous humor (Aq), and vitreous humor (Vit), together with the application of topical and intravitreal treatments (the tear film and representations of treatment are not to scale). (Top panel created in https://BioRender.com/i25q634.) *Bottom*: schematic diagram, summarizing the movement of v (V), r (R), u (VR), and w (RVR) between compartments; their reactions ($\rightleftharpoons$) and degradation ($\rightarrow \emptyset$) within compartments; and the dynamic tear volume, V_{Tear} (see Table 2 for a full list of model variables). Parameters: $\beta_{\text{Tear-Aq},r}$ (cm h^{-1}), the permeability of the tear-aqueous interface to R with CPP; $\beta_{\text{Aq-Vit},j}$ (cm h^{-1}), for $j \in \{v, r, u, w\}$, the permeability of the aqueous-vitreous interface to V/R/VR/RVR; $\beta_{\text{Vit-Ret},\tilde{j}}$ (cm h^{-1}), for $\tilde{j} \in \{r, u, w\}$, the permeability of the vitreo-retinal interface to R/VR/RVR; ψ_{Tear} (mL h^{-1}), the rate of fluid inflow/outflow to/from the tear film (causing dilution of R); ψ_{Aq} (mL h^{-1}), the rate of fluid inflow/outflow to/from the aqueous (causing dilution of V, R, VR, and RVR); and $\phi_{\text{Vit},v}$ (pmol h^{-1}), the rate at which the retina contributes V to the vitreous (see Table 3 for a full list of model parameters and their values).

Investigative Ophthalmology & Visual Science

Downloaded from iovs.arvojournals.org on 09/24/2025

volume, is $V_{\text{Tear}_{\text{Res}}} = 3 \times 10^{-2}$ mL. Therefore, following the application of an eye drop, the tear volume increases to $V_{\text{Tear}_{\text{Res}}}$, while the remaining liquid (with a volume equal to $V_{\text{Tear}_{\text{Norm}}} + V_{\text{Drop}} - V_{\text{Tear}_{\text{Res}}} = 2.14 \times 10^{-2}$ mL) flows immediately off of the eye. While $V_{\text{Tear}}(t) > V_{\text{Tear}_{\text{Norm}}}$, the rate of tear drainage exceeds that of the inflow, such that $V_{\text{Tear}}(t)$ returns to $V_{\text{Tear}_{\text{Norm}}}$ in time τ_{loss} (h), where we assume that volume reduction proceeds linearly. Thus, we have the following algebraic equations for tear film volume:

$$V_{\text{Tear}}(t) = \begin{cases} \underbrace{V_{\text{Tear}_{\text{Norm}}}}_{\text{normal volume}} \text{ constant}, \\ \underbrace{V_{\text{Tear}_{\text{Norm}}}}_{\text{normal volume}} + \underbrace{(V_{\text{Tear}_{\text{Res}}} - V_{\text{Tear}_{\text{Norm}}})\left(1 - \frac{t}{\tau_{\text{loss}}}\right) H(\tau_{\text{loss}} - t)}_{\text{drainage}} \text{ depleting}, \end{cases} \tag{2}$$

where $H(\cdot)$ is the Heaviside step function, defined as

$$H(x) := \begin{cases} 0 & \text{if } x < 0, \\ 1 & \text{if } x \geq 0, \end{cases}$$

which is required to prevent $V_{\text{Tear}}(t)$ going below $V_{\text{Tear}_{\text{Norm}}}$ when $t > \tau_{\text{loss}}$.

The tear film ranibizumab concentration, $r_{\text{Tear}}(t)$ (pmol mL^{-1}), is assumed to be fixed in the drug-eluting contact lens case, such that the rate of change of r_{Tear} over time, $\frac{dr_{\text{Tear}}}{dt}$, is zero. While, in the drop-based therapy case, r_{Tear} decreases over time due to its diffusion across the cornea into the aqueous and due to dilution of the tear film as new fluid is added and old fluid is drained away (ranibizumab is assumed to be too large and hydrophilic to pass across the conjunctiva). VEGF concentrations in the human tear film have been measured to lie in the range 7.48×10^{-4} to 3.08×10^{-1} pmol mL^{-1} across healthy individuals and patients with AMD,[34–36] around five to seven orders of magnitude smaller than the tear ranibizumab concentration following topical application, $r_{\text{Tear}_{\text{init}}} = 1.81 \times 10^{4}$ pmol mL^{-1} (see Appendix A: Parameter Justification). Therefore, we neglect VEGF and its compounds (V, VR, and RVR) in the tear film. We assume that CPPs aid only the passage of ranibizumab, and only then in passing from the tear film to the aqueous. Therefore, we assume that V, VR, and RVR cannot pass across the cornea and that the flux of ranibizumab across the cornea depends only upon its concentration in the tear film and not upon its concentration in the aqueous. Given that the volume of the tear film ($V_{\text{Tear}_{\text{Norm}}} = 6.35 \times 10^{-3}$ mL) is over an order of magnitude smaller than that of the aqueous ($V_{\text{Aq}} = 0.16$ mL), we anticipate that the effect of the inclusion of these additional fluxes upon aqueous chemical concentrations would be negligible in any case. Thus, we have the following equation:

$$\frac{dr_{\text{Tear}}}{dt} = \begin{cases} 0 \text{ constant}, \\ -\underbrace{\frac{\beta_{\text{Tear-Aq},r} A_{\text{Tear-Aq}}}{V_{\text{Tear}}(t)} r_{\text{Tear}}}_{\text{loss to Aq}} - \underbrace{\frac{\psi_{\text{Tear}}}{V_{\text{Tear}}(t)} r_{\text{Tear}}}_{\text{dilution}} \text{ depleting}, \end{cases} \tag{3}$$

where $\beta_{\text{Tear-Aq},r}$ (cm h^{-1}) is the permeability of the cornea to ranibizumab (in the presence of CPPs), ψ_{Tear} (mL h^{-1}) is both the rate of tear film production and the rate of tear film drainage (when $V_{\text{Tear}}(t) = V_{\text{Tear}_{\text{Norm}}}$), and $A_{\text{Tear-Aq}}$ (cm^2) is the corneal area (that is, the area of the Tear-Aq interface).

Aqueous (Aq) Compartment. We describe the evolving concentrations of all four biomolecules in the aqueous: V, $v_{\text{Aq}}(t)$ (pmol mL^{-1}), R, $r_{\text{Aq}}(t)$ (pmol mL^{-1}), VR, $u_{\text{Aq}}(t)$ (pmol mL^{-1}), and RVR, $w_{\text{Aq}}(t)$ (pmol mL^{-1}). The dynamics of these biomolecules are governed by their reaction kinetics (Equations 1a–1b) and the law of mass action (which states that the rate of a reaction is directly proportional to the product of the concentrations of the reactants),[37] their decay(/biological degradation), influx from the tear film (through the cornea; R only), exchange with the vitreous (through the suspensory ligaments/zonule, via diffusive flux), and dilution (through production and drainage of the aqueous humor). (Current evidence suggests that aqueous fluid may flow posteriorly, into the vitreous.[38] Given that the rate of flow has yet to be determined,[38] we neglect it here, noting that its inclusion would both increase delivery of topically applied ranibizumab to the posterior segment and reduce ranibizumab loss from the vitreous following intravitreal injection. Ranibizumab is assumed to be too large and hydrophilic to pass across the blood vessel endothelia in the iris and ciliary body.) This gives rise to the following equations:

$$\frac{dv_{\text{Aq}}}{dt} = \underbrace{k^- u_{\text{Aq}} - 2k^+ v_{\text{Aq}} r_{\text{Aq}}}_{\text{reaction kinetics 1a}} - \underbrace{\delta_{\text{Aq},v} v_{\text{Aq}}}_{\text{decay}} + \underbrace{\frac{\beta_{\text{Aq-Vit},v} A_{\text{Aq-Vit}}}{V_{\text{Aq}}}(v_{\text{Vit}} - v_{\text{Aq}})}_{\text{exchange with Vit}} - \underbrace{\frac{\psi_{\text{Aq}}}{V_{\text{Aq}}} v_{\text{Aq}}}_{\text{dilution}}, \tag{4}$$

$$\frac{dr_{\text{Aq}}}{dt} = \underbrace{k^- u_{\text{Aq}} - 2k^+ v_{\text{Aq}} r_{\text{Aq}}}_{\text{reaction kinetics 1a}} + \underbrace{2k^- w_{\text{Aq}} - k^+ r_{\text{Aq}} u_{\text{Aq}}}_{\text{reaction kinetics 1b}} - \underbrace{\delta_{\text{Aq},r} r_{\text{Aq}}}_{\text{decay}} + \underbrace{\frac{\beta_{\text{Tear-Aq},r} A_{\text{Tear-Aq}}}{V_{\text{Aq}}} r_{\text{Tear}}}_{\text{gain from Tear}} + \underbrace{\frac{\beta_{\text{Aq-Vit},r} A_{\text{Aq-Vit}}}{V_{\text{Aq}}}(r_{\text{Vit}} - r_{\text{Aq}})}_{\text{exchange with Vit}} - \underbrace{\frac{\psi_{\text{Aq}}}{V_{\text{Aq}}} r_{\text{Aq}}}_{\text{dilution}}, \tag{5}$$

$$\frac{du_{\text{Aq}}}{dt} = -\underbrace{k^- u_{\text{Aq}} + 2k^+ v_{\text{Aq}} r_{\text{Aq}}}_{\text{reaction kinetics 1a}} + \underbrace{2k^- w_{\text{Aq}} - k^+ r_{\text{Aq}} u_{\text{Aq}}}_{\text{reaction kinetics 1b}} - \underbrace{\delta_{\text{Aq},u} u_{\text{Aq}}}_{\text{decay}} + \underbrace{\frac{\beta_{\text{Aq-Vit},u} A_{\text{Aq-Vit}}}{V_{\text{Aq}}}(u_{\text{Vit}} - u_{\text{Aq}})}_{\text{exchange with Vit}} - \underbrace{\frac{\psi_{\text{Aq}}}{V_{\text{Aq}}} u_{\text{Aq}}}_{\text{dilution}}, \tag{6}$$

$$\frac{dw_{\text{Aq}}}{dt} = -\underbrace{2k^- w_{\text{Aq}} + k^+ r_{\text{Aq}} u_{\text{Aq}}}_{\text{reaction kinetics 1b}} - \underbrace{\delta_{\text{Aq},w} w_{\text{Aq}}}_{\text{decay}} + \underbrace{\frac{\beta_{\text{Aq-Vit},w} A_{\text{Aq-Vit}}}{V_{\text{Aq}}}(w_{\text{Vit}} - w_{\text{Aq}})}_{\text{exchange with Vit}} - \underbrace{\frac{\psi_{\text{Aq}}}{V_{\text{Aq}}} w_{\text{Aq}}}_{\text{dilution}}, \tag{7}$$

where $\delta_{\text{Aq},j}$ (h^{-1}) is the rate of molecular degradation of $j \in \{v, r, u, w\}$ in the aqueous, $\beta_{\text{Aq-Vit},j}$ (cm h^{-1}) is the permeability of the aqueous-vitreous interface (suspensory ligaments) to $j \in \{v, r, u, w\}$, ψ_{Aq} (mL h^{-1}) is the rate of inflow(/outflow) of aqueous humor to(/from) the anterior segment, V_{Aq} (mL) is the aqueous volume, and $A_{\text{Aq-Vit}}$ (cm^2) is the area of the aqueous-vitreous interface.

Vitreal (Vit) Compartment. We describe the evolving concentrations of all four biomolecules in the vitreous: V, $v_{\text{Vit}}(t)$ (pmol mL^{-1}), R, $r_{\text{Vit}}(t)$ (pmol mL^{-1}), VR, $u_{\text{Vit}}(t)$ (pmol mL^{-1}), and RVR, $w_{\text{Vit}}(t)$ (pmol mL^{-1}). As in the aqueous, the dynamics of these biomolecules are governed by their reaction kinetics, their decay(/biological degradation), and their

Investigative Ophthalmology & Visual Science

Downloaded from iovs.arvojournals.org on 09/24/2025

exchange between the aqueous and vitreous. In addition, R, VR, and RVR are lost to the retinal/choroidal tissue via diffusive flux, and V is gained from the retina, where it is produced by the retinal pigment epithelium (RPE). Consequently, we have the following equations:

$$\frac{dv_{Vit}}{dt} = \underbrace{k^- u_{Vit} - 2k^+ v_{Vit} r_{Vit}}_{\text{reaction kinetics 1a}} - \underbrace{\delta_{Vit,v} v_{Vit}}_{\text{decay}} - \underbrace{\frac{\beta_{Aq-Vit,v} A_{Aq-Vit}}{V_{Vit}}(v_{Vit} - v_{Aq})}_{\text{exchange with Aq}} + \underbrace{\frac{\phi_{Vit,v}}{V_{Vit}}}_{\text{gain from Ret}}, \quad (8)$$

$$\frac{dr_{Vit}}{dt} = \underbrace{k^- u_{Vit} - 2k^+ v_{Vit} r_{Vit}}_{\text{reaction kinetics 1a}} + \underbrace{2k^- w_{Vit} - k^+ r_{Vit} u_{Vit}}_{\text{reaction kinetics 1b}} - \underbrace{\delta_{Vit,r} r_{Vit}}_{\text{decay}} - \underbrace{\frac{\beta_{Aq-Vit,r} A_{Aq-Vit}}{V_{Vit}}(r_{Vit} - r_{Aq})}_{\text{exchange with Aq}} + \underbrace{\frac{\beta_{Vit-Ret,r} A_{Vit-Ret}}{V_{Vit}} r_{Vit}}_{\text{loss to Ret/Ch}}, \quad (9)$$

$$\frac{du_{Vit}}{dt} = \underbrace{-k^- u_{Vit} + 2k^+ v_{Vit} r_{Vit}}_{\text{reaction kinetics 1a}} + \underbrace{2k^- w_{Vit} - k^+ r_{Vit} u_{Vit}}_{\text{reaction kinetics 1b}} - \underbrace{\delta_{Vit,u} u_{Vit}}_{\text{decay}} - \underbrace{\frac{\beta_{Aq-Vit,u} A_{Aq-Vit}}{V_{Vit}}(u_{Vit} - u_{Aq})}_{\text{exchange with Aq}} + \underbrace{\frac{\beta_{Vit-Ret,u} A_{Vit-Ret}}{V_{Vit}} u_{Vit}}_{\text{loss to Ret/Ch}}, \quad (10)$$

$$\frac{dw_{Vit}}{dt} = \underbrace{-2k^- w_{Vit} + k^+ r_{Vit} u_{Vit}}_{\text{reaction kinetics 1b}} - \underbrace{\delta_{Vit,w} w_{Vit}}_{\text{decay}} - \underbrace{\frac{\beta_{Aq-Vit,w} A_{Aq-Vit}}{V_{Vit}}(w_{Vit} - w_{Aq})}_{\text{exchange with Aq}} + \underbrace{\frac{\beta_{Vit-Ret,w} A_{Vit-Ret}}{V_{Vit}} w_{Vit}}_{\text{loss to Ret/Ch}}, \quad (11)$$

where $\delta_{Vit,j}$ (h^{-1}) is the rate of molecular degradation of $j \in \{v, r, u, w\}$ in the vitreous, $\beta_{Vit\text{-}Ret,j}$ (cm h^{-1}) is the permeability of the vitreo-retinal interface (inner limiting membrane) to $j \in \{r, u, w\}$, $\phi_{Vit,v}$ (pmol h^{-1}) is the rate at which the retina contributes VEGF (produced by the RPE) to the vitreous, V_{Vit} (mL) is the vitreal volume, and $A_{Vit\text{-}Ret}$ (cm^2) is the area of the vitreo-retinal interface (inner limiting membrane). The loss to the retina/choroid terms are taken to depend only upon the R/VR/RVR concentration in the vitreous since the choroidal blood flow quickly removes these species.

Initial Conditions. In addition to the governing equations given above (Equations 2–11), we impose the following initial conditions to fully define our model:

$$\begin{array}{llll} V_{Tear}(0) = V_{Tear_{Norm}} \text{ or } V_{Tear_{Res}}, & r_{Tear}(0) = 0 \text{ or } r_{Tear_{init}}, & & \\ v_{Aq}(0) = 0 \text{ or } v_{Aq_{init}}, & r_{Aq}(0) = 0, & u_{Aq}(0) = 0, & w_{Aq}(0) = 0, \\ v_{Vit}(0) = 0 \text{ or } v_{Vit_{init}}, & r_{Vit}(0) = 0 \text{ or } r_{Vit_{init}}, & u_{Vit}(0) = 0, & w_{Vit}(0) = 0, \end{array} \quad (12)$$

where $r_{Tear_{init}}$ (pmol mL^{-1}), $v_{Aq_{init}}$ (pmol mL^{-1}), $v_{Vit_{init}}$ (pmol mL^{-1}), and $r_{Vit_{init}}$ (pmol mL^{-1}) are positive constants. In the case where an eye drop is applied at $t = 0$ h, the initial tear volume is $V_{Tear_{Res}}$; otherwise, $V_{Tear}(0) = V_{Tear_{Norm}}$ (technically, the tear volume does not require an initial condition, since it is defined by an algebraic equation; however, we include it here for completeness and clarity). For an initial topical treatment (drops or contact lenses), the initial tear ranibizumab concentration $r_{Tear}(0) = r_{Tear_{init}}$, while without topical treatment, $r_{Tear}(0) = 0$. Similarly, for an initial intravitreal treatment, the initial vitreal ranibizumab concentration is $r_{Vit_{init}}$, while without intravitreal treatment, $r_{Vit}(0) = 0$. Treatment is never applied directly to the aqueous; hence, $r_{Aq}(0) = 0$. The initial aqueous and vitreal VEGF concentrations, $v_{Aq_{init}}$ and $v_{Vit_{init}}$, are chosen to be the steady-state VEGF concentrations in the absence of ranibizumab treatment. Finally, the initial concentrations of VR and RVR are chosen to be zero, since ranibizumab has not yet had an opportunity to interact with VEGF. See Table 3 for a full list of model parameters (fixed quantities) and Appendix A: Parameter Justification for a description of how each parameter value was determined.

Cases and Submodels. We use our mathematical model to consider a number of cases, resulting in a series of submodels. Submodels of the ex vivo porcine eye concern treatment with either a single topical drop or a single intravitreal injection (at $t = 0$ h). Submodels of the in vivo human eye span treatments with a single topical drop, a single drug-eluting contact lens, or a single intravitreal injection (at $t = 0$ h); repeated dosing with a single mode of administration (topical drops, drug-eluting contact lenses, or intravitreal injections); and repeated dosing using multiple modes of administration (topical drops and intravitreal injections, or drug-eluting contact lenses and intravitreal injections).

In what follows, we explain how our mathematical model differs between the in vivo human eye and the ex vivo porcine eye, and under each treatment condition, for scenarios in which at most a single dose is applied (at $t = 0$ h; see Repeated Dosing section below for repeated dosing scenarios). The mathematical model of the ex vivo porcine eye was used to obtain fits for the tear-aqueous and aqueous-vitreous interface permeability parameters ($\beta_{Tear\text{-}Aq,r}$ and $\beta_{Aq\text{-}Vit,r}$ respectively), while the model of the in vivo human eye was used to predict how ranibizumab would behave in the human eye, using permeability parameters extrapolated from these fits. For topical treatment simulations, we assume that ranibizumab is applied together with CPPs, while for intravitreal treatment simulations, we assume that ranibizumab is applied without CPPs.

We start by describing in vivo human eye models. For treatment with a drug-eluting contact lens, the model is as stated in Equations 2–12, taking the first option in Equations 2 and 3, such that $V_{Tear} = V_{Tear_{Norm}}$ and $r_{Tear} = r_{Tear_{init}}$ are constants, and choosing $v_{Aq}(0) = v_{Aq_{init}}$, $v_{Vit}(0) = v_{Vit_{init}}$, and $r_{Vit}(0) = 0$. For drop-based therapy, the model is as stated in Equations 2–12, taking the second option in Equations 2 and 3, and choosing $V_{Tear}(0) = V_{Tear_{Res}}$, $r_{Tear}(0) = r_{Tear_{init}}$, $v_{Aq}(0) = v_{Aq_{init}}$, $v_{Vit}(0) = v_{Vit_{init}}$, and $r_{Vit}(0) = 0$. For an intravitreal injection, equations concerned with the tear film are removed (Equations 2 and 3), together with their associated dependent variables (V_{Tear} and r_{Tear}) and initial conditions (Equation 12, top line), as is the gain from tear film term from Equation 5, while $v_{Aq}(0) = v_{Aq_{init}}$, $v_{Vit}(0) = v_{Vit_{init}}$, and $r_{Vit}(0) = r_{Vit_{init}}$.

Next, we consider models of the ex vivo porcine eye. For drop-based therapy, the model is similar to that for

Investigative Ophthalmology & Visual Science

Downloaded from iovs.arvojournals.org on 09/24/2025

Table 3. Parameter Values Used in the Mathematical Models (See Equations 2–13), Given to a Maximum of Three Significant Figures

Parameter	Description	Value	Source
τ_{loss}	Time for tear volume to return to normal (human)/zero (porcine)	5.00×10^{-2} h 5.00×10^{-2} h	39–43 This study and 39–43
V_{Drop}	Volume of eye drop	4.50×10^{-2} mL	This study
$V_{\text{Tear}_{\text{Norm}}}$	Volume of normal tear film	6.35×10^{-3} mL N/A	44, 45 —
$V_{\text{Tear}_{\text{Res}}}$	Volume of tear reservoir	3.00×10^{-2} mL N/A	40, 42, 46, 47 —
V_{Aq}	Volume of aqueous	0.160 mL 0.310 mL	48 49, 50
V_{Vit}	Volume of vitreous	4.50 mL 3.10 mL	17, 49, 51, 52 49, 50, 53, 54
$A_{\text{Tear-Aq}}$	Area of the tear-aqueous interface	1.30 cm^2 1.51 cm^2	Calculated from data in 55, 56 Calculated from data in this study and 57
$A_{\text{Aq-Vit}}$	Area of the aqueous-vitreous interface	0.349 cm^2 0.301 cm^2	Calculated from data in 58 Calculated from data in 55, 57, 59–64
$A_{\text{Vit-Ret}}$	Area of the vitreo-retinal interface	10.9 cm^2 N/A	Calculated from data in 65 —
k^+	Binding rate of R to VR (to form RVR)	0.576 pmol^{-1} mL h^{-1}	66
k^-	Unbinding rate of VR (to form V + R)	2.63×10^{-2} h^{-1}	66
$\delta_{i,j}$	Rate of molecular degradation ($i \in$ {Aq, Vit} and $j \in \{v, r, u, w\}$)	0 h^{-1}	Simplifying assumption
$\beta_{\text{Tear-Aq},r}$	Permeability of the tear-aqueous interface to R with CPP	1.10×10^{-6} cm h^{-1} 5.93×10^{-7} cm h^{-1}	Inferred from porcine value using data in 24, 55, 59, 64 Model fit
$\beta_{\text{Aq-Vit},v}$	Permeability of the aqueous-vitreous interface to V	0.985 cm h^{-1}	Inferred from $\beta_{\text{Aq-Vit},r}$ using data in 17, 67, 68
$\beta_{\text{Aq-Vit},r}$	Permeability of the aqueous-vitreous interface to R	0.929 cm h^{-1}	Model fit
$\beta_{\text{Aq-Vit},u}$	Permeability of the aqueous-vitreous interface to VR	0.755 cm h^{-1}	Inferred from $\beta_{\text{Aq-Vit},r}$ using data in 17, 67, 68
$\beta_{\text{Aq-Vit},w}$	Permeability of the aqueous-vitreous interface to RVR	0.653 cm h^{-1}	Inferred from $\beta_{\text{Aq-Vit},r}$ using data in 17, 67, 68
$\beta_{\text{Vit-Ret},r}$	Permeability of the vitreo-retinal interface to R	6.80×10^{-4} cm h^{-1} 0 cm h^{-1}	19 —
$\beta_{\text{Vit-Ret},u}$	Permeability of the vitreo-retinal interface to VR	6.44×10^{-4} cm h^{-1} 0 cm h^{-1}	19 —
$\beta_{\text{Vit-Ret},w}$	Permeability of the vitreo-retinal interface to RVR	6.23×10^{-4} cm h^{-1} 0 cm h^{-1}	19 —
$\phi_{\text{Vit},v}$	Rate at which retina contributes V to vitreous	2.34×10^{-4} pmol h^{-1} 0 pmol h^{-1}	Mean value from 17 —
ψ_{Tear}	Rate of inflow/outflow to/from tear film	7.20×10^{-2} mL h^{-1} 0 mL h^{-1}	44 —
ψ_{Aq}	Rate of inflow/outflow to/from aqueous	0.150 mL h^{-1} 0 mL h^{-1}	17, 24, 69, 70 —
$v_{\text{Aq}_{\text{init}}}$	Initial V concentration in aqueous	1.56×10^{-3} pmol mL^{-1} 0 pmol mL^{-1}	Model steady-state without R Simplifying assumption/this study
$v_{\text{Vit}_{\text{init}}}$	Initial V concentration in vitreous	2.24×10^{-3} pmol mL^{-1} 0 pmol mL^{-1}	Model steady-state without R Simplifying assumption/this study
r_{Dose}	R dose concentration	2.07×10^{4} pmol mL^{-1}	This study and 17, 67
$r_{\text{Tear}_{\text{init}}}$	Initial R concentration in tear	1.81×10^{4} pmol mL^{-1} 2.07×10^{4} pmol mL^{-1}	Calculated Calculated
$r_{\text{Vit}_{\text{init}}}$	Initial R concentration in vitreous	2.07×10^{2} pmol mL^{-1} 4.29 pmol mL^{-1}	Calculated This study

Parameters are fixed quantities that do not change during a simulation.

Where a single value is given, this holds for both human and porcine eyes. Where two values are given, the first is for human eyes and the second is for porcine eyes. See Appendix A: Parameter Justification for a description of how each parameter value was determined.

the in vivo human eye (above), but with the following modifications—we replace Equation 2 with Equation 13 (below), and $V_{\text{Tear}}(0) = V_{\text{Drop}}$. We also modify the parameters (see Table 3); in particular, $\psi_{\text{Tear}} = 0$, $\psi_{\text{Aq}} = 0$, $\phi_{\text{Vit},v} = 0$, and $\beta_{\text{Vit-Ret},j} = 0$ for $j \in \{r, u, w\}$, since there is no tear or aqueous production/drainage and no VEGF production or choroidal blood flow in an ex vivo eye. For an intravitreal injection, the model is the same as for the in vivo human eye (above), but with modified parameters (see Table 3). In particular, $\psi_{\text{Aq}} = 0$, $\phi_{\text{Vit},v} = 0$, and $\beta_{\text{Vit-Ret},j} = 0$ for $j \in \{r, u, w\}$, since there is no aqueous production/drainage, VEGF production, or choroidal blood flow in an ex vivo eye.

Investigative Ophthalmology & Visual Science

Downloaded from iovs.arvojournals.org on 09/24/2025

We consider two forms for the tear volume equation in the ex vivo porcine eye: a *depleting volume* case, in which the drop flows off of the cornea in time τ_{loss} (linearly, as with the in vivo human eye), and the limiting, *constant volume* case, where the full drop remains on the cornea throughout the experiment. This gives rise to the following equations:

$$V_{\text{Tear}}(t) = \begin{cases} \underbrace{V_{\text{Drop}}}_{\substack{\text{drop}\\\text{volume}}} \text{ constant (ex vivo porcine)}, \\ \underbrace{V_{\text{Drop}}\left(1 - \frac{t}{\tau_{\text{loss}}}\right) H(\tau_{\text{loss}} - t)}_{\text{runoff}} \text{ depleting (ex vivo porcine)}, \end{cases} \tag{13}$$

where the full drop volume is lost in the volume loss case since a tear film cannot be maintained in the absence of the surrounding tissues. We consider both constant volume and volume loss cases since it is impractical to precisely characterize the time for a drop to flow off of the cornea (visual observation suggests that the majority of the drop volume remains on the cornea during the experiment), and to allow us to assess the influence of the rate of drop volume loss when fitting other parameters to the experimental data (see Model Fitting below).

Repeated Dosing. Alongside the single-dose scenario, we also consider repeated dosing for drop, contact lens, and intravitreal treatments in the in vivo human eye. In this case, the initial conditions given in Equation 12 hold only for the initial time interval (that is, the interval before the second dose is applied if the first is applied at $t = 0$ h, or the interval before the first dose is applied otherwise). For each dose applied after $t = 0$ h, we solve the governing Equations 2–11 up to the time at which the new dose is applied, $t = t_{\text{dose}_n}$ h, say, at which point we modify the relevant dependent variables to account for the new treatment, which provides the initial conditions for the next time interval, $t \in (t_{\text{dose}_n}, t_{\text{dose}_{n+1}}]$.

Upon the application of a drop, $V_{\text{Tear}}(t)$ jumps from $V_{\text{Tear}_{\text{Norm}}}$ to $V_{\text{Tear}_{\text{Res}}}$, with the excess volume ($V_{\text{Tear}_{\text{Norm}}} + V_{\text{Drop}} - V_{\text{Tear}_{\text{Res}}}$) flowing immediately off of the eye. With the exception of r_{Tear} and/or r_{Vit}, the initial conditions for each biochemical dependent variable are equal to their values at the final time point in the previous treatment interval. Upon application of a drop/contact lens and/or intravitreal treatment, the initial conditions for r_{Tear} and/or r_{Vit}, respectively, will be discontinuous with their values at the final time point in the previous treatment interval, with new values calculated as follows.

When a new eye drop is applied, the fluid in the drop immediately merges and mixes with the fluid in the tear film, such that $r_{\text{Tear}_{\text{New}}} = \frac{r_{\text{Tear}_{\text{Old}}} V_{\text{Tear}_{\text{Norm}}}}{V_{\text{Tear}_{\text{Norm}}} + V_{\text{Drop}}} + \frac{r_{\text{Dose}} V_{\text{Drop}}}{V_{\text{Tear}_{\text{Norm}}} + V_{\text{Drop}}}$, where $r_{\text{Tear}_{\text{New}}}$ (pmol mL^{-1}) is the tear film ranibizumab concentration immediately after the application of a drop, $r_{\text{Tear}_{\text{Old}}}$ (pmol mL^{-1}) is the tear film ranibizumab concentration immediately before the application of a drop, and r_{Dose} (pmol mL^{-1}) is the ranibizumab concentration within the drop, prior to application. Thus, the mixing is assumed to occur sufficient rapidly that the ranibizumab concentration equilibrates throughout the tear film/drop, prior to the excess volume ($V_{\text{Tear}_{\text{Norm}}} + V_{\text{Drop}} - V_{\text{Tear}_{\text{Res}}}$) leaving the tear film. If the previous treatment at $t_{\text{dose}_{n-1}}$ was also in the form of an eye drop, then we choose t_{dose_n} such that $t_{\text{dose}_n} - t_{\text{dose}_{n-1}} \geq \tau_{\text{loss}}$, ensuring that $V_{\text{Tear}}(t)$ has returned to $V_{\text{Tear}_{\text{Norm}}}$ when the new drop is applied.

When a new drug-eluting contact lens is inserted, it is assumed that the tear ranibizumab concentration immediately takes a value of $r_{\text{Tear}_{\text{init}}}$ and that this is maintained throughout the period for which it is worn. Upon removal of the contact lens, the tear ranibizumab concentration decays as described by the depleting form of Equation 3.

When a new intravitreal injection is administered, it is assumed that the ranibizumab concentration quickly equilibrates throughout the vitreous, such that $r_{\text{Vit}_{\text{New}}} = r_{\text{Vit}_{\text{Old}}} + \frac{r_{\text{Dose}} V_{\text{Drop}}}{V_{\text{Vit}}}$, where $r_{\text{Vit}_{\text{New}}}$ (pmol mL^{-1}) is the vitreal ranibizumab concentration immediately after the application of an injection, and $r_{\text{Vit}_{\text{Old}}}$ (pmol mL^{-1}) is the vitreal ranibizumab concentration immediately before the application of an injection (the injected volume is the same as the drop volume, hence we use the same parameter, V_{Drop}, for both). It is assumed that the injected volume does not affect the vitreal volume, the additional volume being negligible (given that $V_{\text{Drop}} \ll V_{\text{Vit}}$) and quickly drained.

We also consider treatment regimens that combine topical (drop and contact lens) and intravitreal doses. In this case, each treatment type follows the rules described above.

In the case where a single dose is applied at $t = 0$ h, time, t, can simply be measured from $t = 0$ h. The situation is a little more complicated in the case of repeated dosing, since solution of the governing Equations 2–11 must be halted and reinitialized for every new dose. As such, it is helpful to distinguish between what we shall term "local" and "global" time. Global time spans the full duration of a simulation and is the time plotted in figures, while local time is the time "seen" by the governing equations and is reset to zero upon the application of each treatment. For notational simplicity, we use t to denote both local and global time, with the local/global distinction being understood from the context in which it is used.

Sensitivity Analysis

A local sensitivity analysis was performed to determine the effect of varying each parameter upon key model outputs. Parameters were varied individually, across 101 values uniformly distributed over the biologically realistic ranges given in Table 4, while keeping all remaining parameters fixed at their default values in Table 4. For each parameter set, Equations 2–12 were solved for $t \in [0, 12]$ weeks and the outputs from the interval $t \in [9, 12]$ weeks—within which the solution has firmly settled to either an unchanging steady-state or a regular periodic pattern—used to calculate the maximum, mean, and minimum vitreal values of V and R_{Tot} (= R + VR + 2RVR, the total ranibizumab concentration; see Supplementary Figs. S2–S7). We choose vitreal values as our key outputs since these are the most relevant in preventing choroidal neovascularization, and calculate the max/mean/min since it is important to minimize all three quantities for VEGF and to maximize all three quantities for R_{Tot}. We use R_{Tot} rather than R since the total quantity of ranibizumab is of greater significance than the free quantity—sensitivity analysis was also performed on R and the results were almost identical to those for R_{Tot}.

For each key output and parameter, we calculate the *sensitivity factor*, defined as the maximum value obtained by the output over the 101 values across which the parameter was varied, divided by the minimum value over that range. Thus, for a given treatment scenario, each parameter has

Investigative Ophthalmology & Visual Science

Downloaded from iovs.arvojournals.org on 09/24/2025

Table 4. Parameter Default Values and Value Ranges for Sensitivity Analysis of the In Vivo Human Model

Parameter	Default Value	Range of Values
τ_{loss}	5.00×10^{-2} h	$[1.67, 8.33] \times 10^{-2}$ h
V_{Drop}	4.50×10^{-2} mL	$[4.05, 4.95] \times 10^{-2}$ mL
$V_{Tear_{Norm}}$	6.35×10^{-3} mL	$[0.340, 1.07] \times 10^{-2}$ mL
$V_{Tear_{Res}}$	3.00×10^{-2} mL	$[2.70, 3.30] \times 10^{-2}$ mL
V_{Aq}	0.160 mL	[0.121, 0.286] mL
V_{Vit}	4.50 mL	[3.50, 5.40] mL
$A_{Tear\text{-}Aq}$	1.30 cm^2	[1.04, 1.56] cm^2
$A_{Aq\text{-}Vit}$	0.349 cm^2	[0.111, 0.521] cm^2
$A_{Vit\text{-}Ret}$	10.9 cm^2	[9.81, 12.0] cm^2
k^+	0.576 $pmol^{-1}$ mL h^{-1}	[0.205, 4.21] $pmol^{-1}$ mL h^{-1}
k^-	2.63×10^{-2} h^{-1}	$[1.40, 3.60] \times 10^{-2}$ h^{-1}
$\delta_{i,j}$ *	0 h^{-1}	[0, 0.770] h^{-1}
$\beta_{Tear\text{-}Aq,r}$	1.10×10^{-6} cm h^{-1}	$[0.990, 1.21] \times 10^{-6}$ cm h^{-1}
$\beta_{Aq\text{-}Vit,v}$	0.985 cm h^{-1}	[0.887, 1.08] cm h^{-1}
$\beta_{Aq\text{-}Vit,r}$	0.929 cm h^{-1}	[0.836, 1.02] cm h^{-1}
$\beta_{Aq\text{-}Vit,u}$	0.755 cm h^{-1}	[0.680, 0.831] cm h^{-1}
$\beta_{Aq\text{-}Vit,w}$	0.653 cm h^{-1}	[0.588, 0.718] cm h^{-1}
$\beta_{Vit\text{-}Ret,r}$	6.80×10^{-4} cm h^{-1}	[6.12, 7.48] $\times 10^{-4}$ cm h^{-1}
$\beta_{Vit\text{-}Ret,u}$	6.44×10^{-4} cm h^{-1}	[5.80, 7.08] $\times 10^{-4}$ cm h^{-1}
$\beta_{Vit\text{-}Ret,w}$	6.23×10^{-4} cm h^{-1}	[5.61, 6.85] $\times 10^{-4}$ cm h^{-1}
$\phi_{Vit,v}$	2.34×10^{-4} pmol h^{-1}	[1.02, 4.46] $\times 10^{-4}$ pmol h^{-1}
ψ_{Tear}	7.20×10^{-2} mL h^{-1}	$[0.300, 1.32] \times 10^{-1}$ mL h^{-1}
ψ_{Aq}	0.150 mL h^{-1}	$[0.660, 2.52] \times 10^{-1}$ mL h^{-1}
r_{Dose}	2.07×10^4 pmol mL^{-1}	$[1.86, 2.28] \times 10^4$ pmol mL^{-1}

See Appendix A: Parameter Justification for an explanation of parameter values.

* For $i \in \{Aq, Vit\}$ and $j \in \{v, r, u, w\}$.

six sensitivity factors associated with it, one for each of the key model outputs (max/mean/min of V/R_{Tot}). We consider a sensitivity factor to be significant if it exceeds 1.5, such that the key model output varies by over 50% of its minimum value within the range of values considered for that parameter. There is no best objective value for this threshold; we chose 1.5 since this represents a substantial variation without being overly stringent.

Results

Porcine Eyes

Experimental Results. Control ranibizumab measurements in the aqueous were 0 pmol mL^{-1}, while those in the vitreous were 0.348 ± 0.459 pmol mL^{-1}, despite ranibizumab being absent. This is likely due to the effects of vitreal proteins being mis-detected as ranibizumab. Control VEGF measurements in the aqueous were $9.87 \times 10^{-3} \pm 1.24 \times 10^{-3}$ pmol mL^{-1}, while those in the vitreous were 0 pmol mL^{-1}. It is unclear why VEGF was not detected in the vitreal controls. Given that VEGF levels in the vitreous for topical therapy (for which vitreal ranibizumab levels are within the range of controls) are at similar levels to the aqueous control values, we assume that vitreal control values should be roughly the same as aqueous control values.

Three treatments were tested: (1) topical treatment with ranibizumab and CPP, (2) intravitreal treatment with ranibizumab and CPP, and (3) intravitreal treatment with ranibizumab alone (see Table 5 for a summary of the experimental results). Treatment 2 acts as a positive control we use to demonstrate that we can detect our molecule of interest (ranibizumab) and also compare against the levels used for topical administration.

First, for topical treatment with ranibizumab and CPP (Fig. 3 [top row]), the aqueous ranibizumab levels increased significantly, versus controls, by 3.5 h ($7.14 \times 10^{-2} \pm 9.46 \times 10^{-2}$ pmol mL^{-1}; $P = 0.03$), coincident with a significant ($P = 0.03$) drop in aqueous VEGF between 1 h ($8.85 \times 10^{-3} \pm 6.06 \times 10^{-4}$ pmol mL^{-1}) and 3.5 h ($6.26 \times 10^{-4} \pm 1.08 \times 10^{-3}$ pmol mL^{-1}). Vitreal ranibizumab increased gradually, with a significant ($P = 0.03$) increase between 40 min ($8.79 \times 10^{-2} \pm 1.80 \times 10^{-2}$ pmol mL^{-1}) and 3.5 h (0.364 ± 0.189 pmol mL^{-1}), though remaining within the range of the controls (0.348 ± 0.459 pmol mL^{-1}), while vitreal VEFG remained constant. The aqueous ranibizumab measurements at 1 hour were all outside the limits of detection (0 pmol mL^{-1}). This was somewhat anomalous given that ranibizumab was detected at all other time points, and thus we neglect this point in the Model Fitting section below.

Table 5. Experimental Results for Treatment of Ex Vivo Porcine Eyes

			Concentration (pmol mL^{-1})			
			20 min	40 min	1 h	3.5 h
Topical with CPP	RBZ	Aq	6.76×10^{-3} (1.17×10^{-2})	3.80×10^{-2} (6.58×10^{-2})	0 (0)	7.14×10^{-2} (9.46×10^{-2})
		Vit	3.66×10^{-2} (1.11×10^{-2})	8.79×10^{-2} (1.80×10^{-2})	0.187 (9.94×10^{-2})	0.364 (0.189)
	VEGF	Aq	8.01×10^{-3} (4.52×10^{-4})	8.08×10^{-3} (1.50×10^{-3})	8.85×10^{-3} (6.06×10^{-4})	6.26×10^{-4} (1.08×10^{-3})
		Vit	7.34×10^{-3} (1.55×10^{-3})	6.59×10^{-3} (1.25×10^{-3})	5.09×10^{-3} (1.59×10^{-3})	7.47×10^{-3} (1.26×10^{-3})
Invit. with CPP	RBZ	Aq	1.39×10^{-2} (0.196)	3.12×10^{-2} (5.41×10^{-2})	2.00×10^{-2} (2.83×10^{-2})	2.63 (1.94)
		Vit	1.30 (0.384)	2.41 (1.29)	2.91 (0.101)	4.40 (4.40×10^{-2})
	VEGF	Aq	9.20×10^{-3} (5.11×10^{-4})	9.53×10^{-3} (4.32×10^{-4})	1.60×10^{-2} (1.10×10^{-2})	6.51×10^{-3} (6.05×10^{-3})
		Vit	2.84×10^{-3} (4.02×10^{-3})	2.11×10^{-3} (1.67×10^{-3})	1.36×10^{-3} (1.23×10^{-3})	5.01×10^{-5} (8.68×10^{-5})
Invit. w/o CPP	RBZ	Aq	4.73×10^{-2} (0)	4.27×10^{-2} (7.40×10^{-2})	0.774 (0.931)	4.35 (1.86×10^{-2})
		Vit	4.29 (0.435)	3.73 (0.186)	4.11 (0.312)	4.47 (0.236)
	VEGF	Aq	8.25×10^{-3} (1.96×10^{-3})	1.23×10^{-2} (6.35×10^{-4})	7.84×10^{-3} (4.31×10^{-3})	6.52×10^{-3} (5.84×10^{-3})
		Vit	6.73×10^{-3} (3.02×10^{-3})	0 (0)	0 (0)	0 (0)
Invit. sterile water control	RBZ	Aq	0 (0)			
		Vit	0.348 (0.459)			
	VEGF	Aq	9.87×10^{-3} (1.24×10^{-3})			
		Vit	0 (0)			

RBZ, ranibizumab.

Controls are not associated with a particular time point (see Experimental methods).

Stated values are means, with standard deviations in parentheses ($n = 3$ for each data point). All values are given to three significant figures. These data are plotted in Figure 3.

Investigative Ophthalmology & Visual Science

Downloaded from iovs.arvojournals.org on 09/24/2025

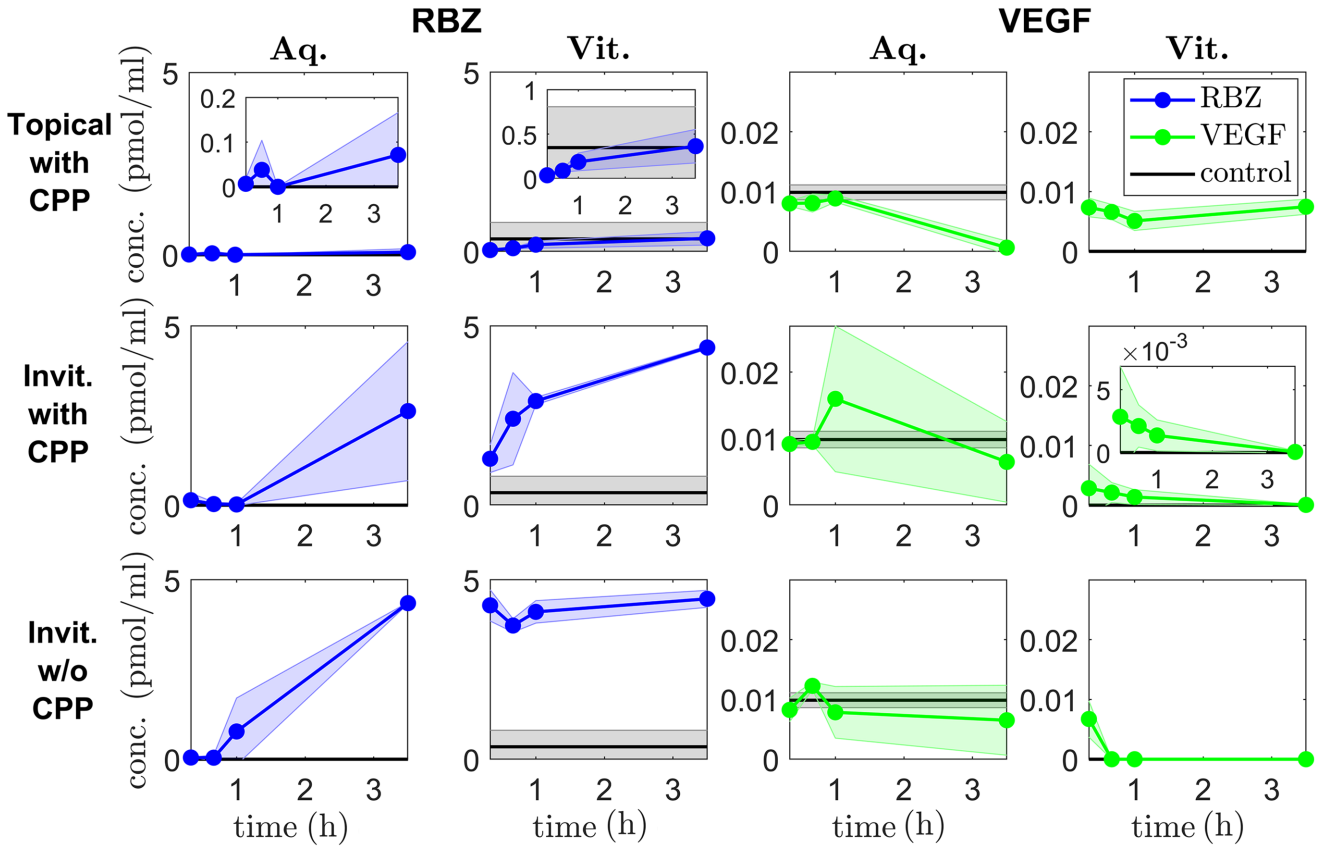

Figure 3. Experimental results for treatment of ex vivo porcine eyes. Panels show ranibizumab (RBZ, *first two columns*) and VEGF (*last two columns*) concentrations in the aqueous (Aq, *columns 1 and 3*) and vitreous (Vit, *columns 2 and 4*), at $t = 20$ min, 40 min, 1 h and 3.5 h. *Top row*: topical treatment (45 µL) with ranibizumab (1 mg mL^{-1}) and CPP (100 mg mL^{-1}). Ranibizumab is detected in significant quantities in the aqueous and appears to enter the vitreous, though it only has a significant effect in reducing aqueous VEGF levels, leaving vitreal VEGF levels unaffected. *Middle row*: intravitreal (invit.) treatment (45 µL) with ranibizumab (1 mg mL^{-1}) and CPP (100 mg mL^{-1}). As expected, vitreal ranibizumab levels are high, resulting in a significant reduction in vitreal VEGF levels. *Bottom row*: intravitreal treatment (45 µL) with ranibizumab only (1 mg mL^{-1}). Interestingly, intravitreal treatment is more effective in reducing vitreal VEGF in the absence of CPPs. See Table 5 for numerical values of data points.

Second, for intravitreal treatment with ranibizumab and CPP (Fig. 3 [middle row]), aqueous ranibizumab was first detected in significant quantities, compared to controls, at 3.5 h (2.63 ± 1.94 pmol mL^{-1}; $P = 0.03$), while aqueous VEFG remained constant. Vitreal ranibizumab increased steadily and significantly ($P = 0.03$) from 20 min (1.30 ± 0.384 pmol mL^{-1}) to 3.5 h (4.40 ± 4.40 × 10^{-2} pmol mL^{-1}), coincident with a significant ($P = 0.03$) drop in vitreal VEGF from 40 min (2.11 × 10^{-3} ± 1.67 × 10^{-3} pmol mL^{-1}) to 3.5 h (5.01 × 10^{-5} ± 8.68 × 10^{-5} pmol mL^{-1}).

Third, for intravitreal treatment with ranibizumab alone (Fig. 3 [bottom row]), aqueous ranibizumab was present in significant quantities, versus controls, by 1 h (0.774 ± 0.931 pmol mL^{-1}; $P = 0.03$), while aqueous VEFG remained constant. Vitreal ranibizumab maintained constant values (∼4 pmol mL^{-1}) for all time points, while vitreal VEGF was undetectable from 40 min onward.

Detected vitreal ranibizumab values following intravitreal ranibizumab injections (with and without CPP) are much lower than would be anticipated based on the injected dose concentration (and volume). Given the injected dose, an initial intravitreal ranibizumab concentration of 3.00 × 10^{2} pmol mL^{-1} would be expected (see Appendix A: Parameter Justification); however, measured vitreal values do not exceed 5 pmol mL^{-1}. It may be that, despite being placed on a shaker, vitreal ranibizumab does not spread out uniformly from the injection site over the time frame of our experiments and that our samples were taken from a portion of the vitreous away from the injection site.

Model Fitting. All ex vivo porcine parameter values were taken or calculated from the literature, or taken directly from our experimental data, except for the permeabilities of the Tear-Aq and Aq-Vit interfaces to ranibizumab, $\beta_{\text{Tear-Aq},r}$ and $\beta_{\text{Aq-Vit},r}$, respectively, which were determined by fitting our mathematical model to the experimental data.

Data from topical drop administration with CPP experiments were used for fitting, for which a single drop is applied at $t = 0$ h. Equations 3–13 were solved with depleting tear ranibizumab concentration, constant tear volume, and in the absence of VEGF. Simulations were initialized at $t = 0$ h with $r_{\text{Tear}}(0) = r_{\text{Dose}} = 2.07 \times 10^4$ pmol mL^{-1}, $r_{\text{Aq}}(0) = 0$ pmol mL^{-1}, and $r_{\text{Vit}}(0) = 0$ pmol mL^{-1}, and the MATLAB (R2020a) routine fminsearch (which uses a Nelder–Mead simplex method) applied (with default settings) to minimize the mean squared error between the data and the model predictions. Fitting was performed for r_{Aq} at $t = 20$ min, 40 min, and 3.5 h to the mean data points, which were deemed to be more accurate than the vitreal ranibizumab measurements, and neglecting the aqueous data point at $t =$ 1 h, which appears anomalous (see Experimental Results).

Investigative Ophthalmology & Visual Science

Downloaded from iovs.arvojournals.org on 09/24/2025

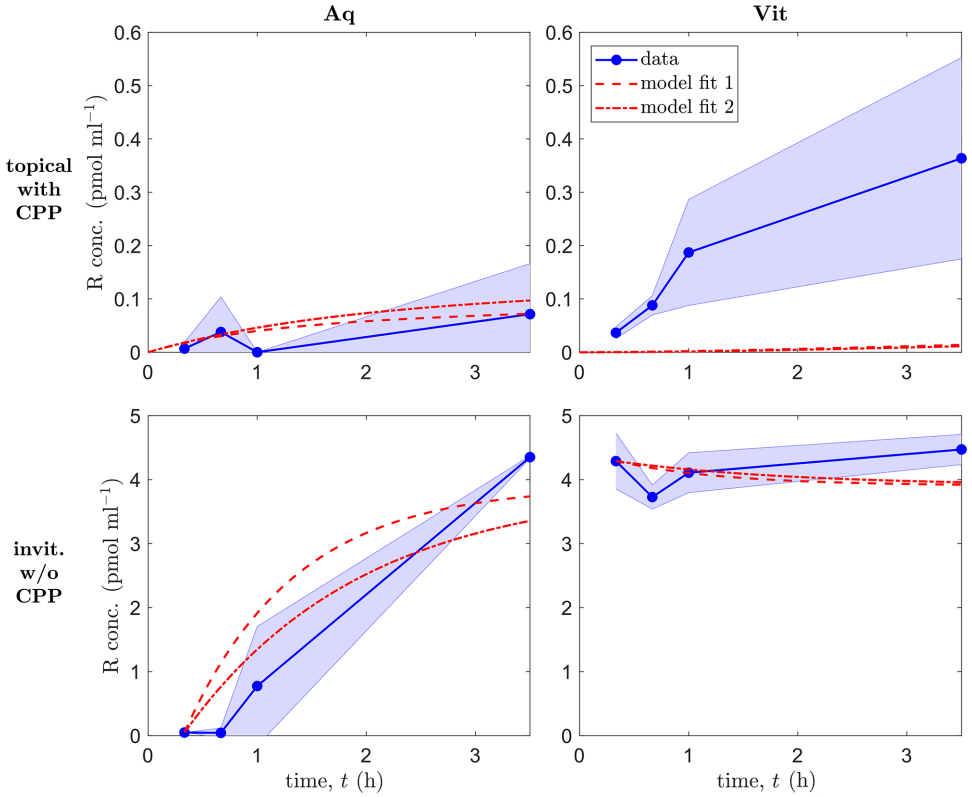

Figure 4. Mathematical model fits to ex vivo porcine data. Panels show ranibizumab (R) concentrations in the aqueous (Aq, *left column*) and vitreous (Vit, *right column*), for topical drop administration with CPPs (*top row*) and for intravitreal injection without CPPs (*bottom row*). *Top row*: a single drop is applied at $t = 0$ h; simulations start at $t = 0$ h with $r_{\text{Tear}}(0) = r_{\text{Dose}} = 2.07 \times 10^4$ pmol mL^{-1}, $r_{\text{Aq}}(0) = 0$ pmol mL^{-1} and $r_{\text{Vit}}(0) = 0$ pmol mL^{-1}; fitting was performed for r_{Aq} at $t = 20$ min, 40 min, and 3.5 h to the mean data points; Equations 3–13 were solved with depleting tear ranibizumab concentration, constant tear volume, and in the absence of VEGF. *Bottom row*: a single injection is administered at $t = 0$ h; simulations start at $t = 20$ min (=1/3 h) with $r_{\text{Aq}}(1/3) = 4.73 \times 10^{-2}$ pmol mL^{-1} and $r_{\text{Vit}}(1/3) = 4.29$ pmol mL^{-1}, equal to the mean data points at those times; fitting was performed for r_{Aq} at $t = 40$ min, 1 h and 3.5 h to the mean data points; Equations 4–12 were solved in the absence of VEGF. Reasonable fits are achieved in all cases except for vitreal ranibizumab with topical treatment. Model fit 1: $\beta_{\text{Tear-Aq},r} = 5.93 \times 10^{-7}$ cm h^{-1} (this value is also used for model fit 2 in the topical case) and $\beta_{\text{Aq-Vit},r} = 0.929$ cm h^{-1}; model fit 2: $\beta_{\text{Aq-Vit},r} = 0.577$ cm h^{-1}. All remaining parameters chosen as the default porcine values in Table 3.

A good fit was achieved in the aqueous (*model fit 1*: $\beta_{\text{Tear-Aq},r} = 5.93 \times 10^{-7}$ cm h^{-1} and $\beta_{\text{Aq-Vit},r} = 0.929$ cm h^{-1}); however, it is not possible to find a good fit in both aqueous and vitreal compartments simultaneously, since measured vitreal ranibizumab concentrations are higher than those in the aqueous, and ranibizumab must move down a concentration gradient from the aqueous to the vitreous for topical treatment (see the top row of Fig. 4).

Another fitting was explored, this time allowing fluid from the drop to flow off of the cornea (the tear volume loss case), and fitting for τ_{loss} in addition to $\beta_{\text{Tear-Aq},r}$ and $\beta_{\text{Aq-Vit},r}$. While a closer fit was obtained than for model fit 1, this would be expected when fitting a greater number of parameters, and the fit requires $\beta_{\text{Aq-Vit},r} \approx 0$ cm h^{-1}, which is unrealistic. Therefore, we consider model fit 1 to be preferable; the unrealistic fit indicates that the majority of the drop volume remains on the cornea during the experiment (a result consistent with our visual observations).

A further fitting was explored to the intravitreal injection without CPPs experimental data, for which a single injection is administered at $t = 0$ h. Equations 4–12 were solved in the absence of VEGF. Simulations were initialized at $t = 20$ min (=1/3 h) with $r_{\text{Aq}}(1/3) = 4.73 \times 10^{-2}$ pmol mL^{-1} and $r_{\text{Vit}}(1/3) = 4.29$ pmol mL^{-1}, equal to the mean data points at those times. We initialize at $t = 20$ min, rather than $t = 0$ h, since the measured vitreal ranibizumab concentrations are lower than would be expected given the injected dose (see the final paragraph of the Experimental Results section for further justification). (These values are also more appropriate, since the measured values are more representative of the vitreal ranibizumab concentration near the aqueous-vitreous interface, given that vitreal mixing has not had a chance to occur by this time point—see our reflection on the well-mixed assumption in the Discussion section.) Fitting was performed for r_{Aq} at $t = 40$ min, 1 h, and 3.5 h to the mean data points, with the aqueous ranibizumab measurements being more informative than the vitreal measurements, which remain roughly constant over time.

A reasonable fit was achieved in the aqueous and vitreous (*model fit 2*: $\beta_{\text{Aq-Vit},r} = 0.577$ cm h^{-1}; see the bottom row of Fig. 4). The fitted value of $\beta_{\text{Aq-Vit},r}$ in model fit 2 is a factor of about 0.62 what it was in model fit 1. We plot simulation results using $\beta_{\text{Aq-Vit},r}$ values from both model fits for both topical and intravitreal treatment (using the model 1 fit value for $\beta_{\text{Tear-Aq},r}$ for model fit 2 in the topical case; Fig. 4). It can be seen that model fit 1 provides a good fit in both cases and actually does a better job in fitting to the $t = 3.5$ h data

Investigative Ophthalmology & Visual Science

Downloaded from iovs.arvojournals.org on 09/24/2025

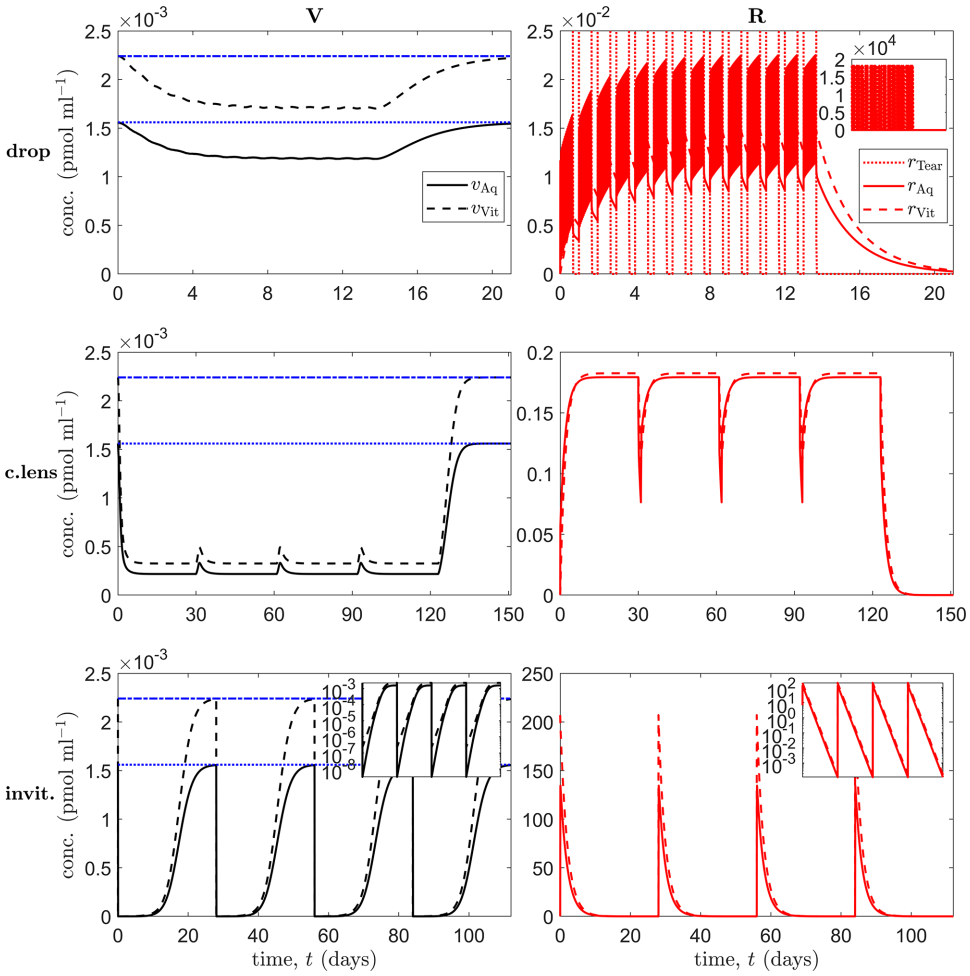

Figure 5. Simulation results for treatment of an in vivo human eye, using a single mode of administration. Panels show VEGF (V) concentrations (*left column*) and ranibizumab (R) concentrations (*right column*) in the tear film (Tear), aqueous (Aq), and vitreous (Vit), as appropriate (insets show results over the full range of concentrations [*top right*], or with a logarithmic scale on the ordinate [*bottom row*]). *Horizontal blue lines* in the left column show untreated VEGF levels in the aqueous (*dotted*) and vitreous (*dash-dot*). *Top row* (topical drops): a single drop is applied at the start of hours 1 to 16 every day for the first 2 weeks; week 3 untreated. *Middle row* (drug-eluting contact lens): a series of four lenses are worn for 30 days at a time, starting on day 1, with a 1-day break between lenses; final 4 weeks untreated. *Bottom row* (intravitreal injections): administered at the start of weeks 1, 5, 9, and 13; simulation runs to 16 weeks. Drops suppress aqueous and vitreal VEGF levels to a fairly constant value during the period of administration; contact lenses suppress VEGF levels more strongly, with small transient increases in VEGF levels between lenses; injections reduce VEGF to by far the lowest levels, though VEGF returns to untreated values between injections. Equations 2–12 were solved using the default human parameters in Table 3.

point in the aqueous for intravitreal treatment than model fit 2. Therefore, we consider model fit 1 to be preferable, taking this as our default for the ex vivo porcine eye.

We repeated each of the above fits, this time including VEGF. As anticipated, the effect on the fitted values was negligible given that VEGF concentrations are at least an order of magnitude lower than ranibizumab concentrations in each compartment.

Finally, we performed a Markov chain Monte Carlo (MCMC) parameter identifiability analysis, employing a Metropolis–Hastings algorithm to determine the uncertainty in our parameter fits for the topical drop administration with CPP and intravitreal injection without CPP cases (model fits 1 and 2, as shown in Fig. 4; with constant tear volume and in the absence of VEGF). The posterior distributions show a single sharp peak for each parameter in all cases, demonstrating that the uncertainty is low (and identifiability is high; see Supplementary Fig. S1). In the topical administration case, $\beta_{\text{Tear-Aq},r}$ has mean 5.93×10^{-7} and standard deviation 2.45×10^{-8}, while $\beta_{\text{Aq-Vit},r}$ has mean 0.930 and standard deviation 6.39×10^{-2}. In the intravitreal administration case, $\beta_{\text{Aq-Vit},r}$ has mean 0.577 and standard deviation 2.75×10^{-2}. See the Supplementary Material for further details.

Human Eyes

Having fitted our model to ex vivo porcine data in the previous section (Model Fitting), we use our model, with appropriate modification of Equations 2–12 and parameters (see Model formulation, Table 3 and Appendix A: Parameter Justification), to predict how ranibizumab will behave in the in vivo human eye and its effect upon VEGF levels.

Model Predictions. We begin by considering treatments involving a single mode of ranibizumab administration, either via topical drops (with CPP) drug-eluting contact lenses (with CPP), or intravitreal injections (without CPP; see Fig. 5), where CPP is not modeled explicitly, but assumed to

Investigative Ophthalmology & Visual Science

Downloaded from iovs.arvojournals.org on 09/24/2025

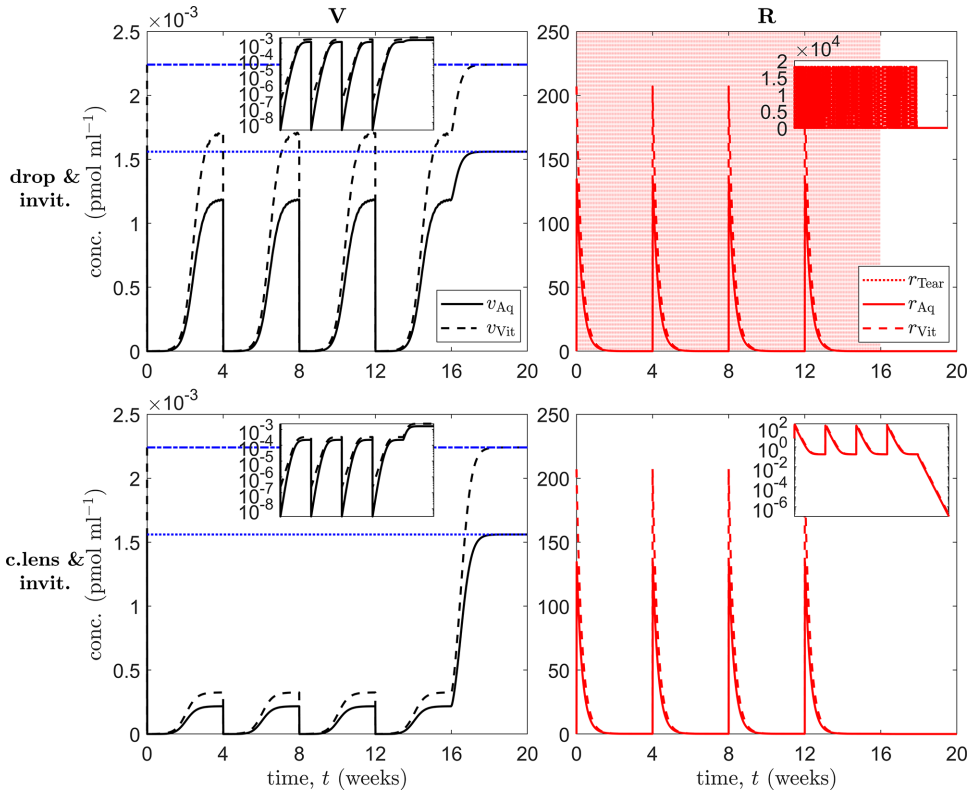

Figure 6. Simulation results for treatment of an in vivo human eye, using multiple modes of administration. Panels show VEGF (V) concentrations (*left column*) and ranibizumab (R) concentrations (*right column*) in the tear film (Tear), aqueous (Aq), and vitreous (Vit), as appropriate (insets show results over the full range of concentrations [*top right*], or with a logarithmic scale on the ordinate [*top left and bottom row*]). *Horizontal blue lines* in the left column show untreated VEGF levels in the aqueous (*dotted*) and vitreous (*dash-dot*). *Top row* (topical drops and intravitreal injections): a single drop is applied at the start of hours 1 to 16 every day for the first 16 weeks, while injections are administered at the start of weeks 1, 5, 9, and 13; simulation runs to 20 weeks, the final 4 untreated. *Bottom row* (drug-eluting contact lens and intravitreal injections): a series of four lenses are worn for 27 days at a time, starting on day 2, with a 1-day break between lenses, while injections are administered at the start of weeks 1, 5, 9, and 13 (on the days without contact lenses); simulation runs to 20 weeks, the final 4 untreated. Both drops and drug-eluting lenses suppress aqueous and vitreal VEGF levels between injections, preventing them from returning to untreated levels as in Figure 5 (*bottom row*). Equations 2–12 were solved using the default human parameters in Table 3.

be present for topical administration to allow ranibizumab to pass through the cornea.

First, in the topical drop case, we consider the scenario where a single drop is applied at the start of hours 1 to 16 every day for the first 2 weeks, with week 3 left untreated (Fig. 5 [top row]). This assumes the patient is awake 16 h a day and applies the treatment once each waking hour. Though four drops a day would be a more realistic maximum frequency,[71] the aim here is to explore the maximum theoretical effect from topical drops. Aqueous and vitreal VEGF levels are suppressed to fairly constant values during the period of administration (1.18×10^{-3} and 1.70×10^{-3} pmol mL^{-1}, respectively), reaching suppressed levels after about 100 h of treatment and returning to untreated values (1.56×10^{-3} and 2.24×10^{-3} pmol mL^{-1}, respectively) after about a week after treatment termination, while aqueous and vitreal ranibizumab concentrations oscillate over ranges of (8.57×10^{-3}, 2.25×10^{-2}) and (1.25×10^{-2}, 1.48×10^{-2}) pmol mL^{-1} respectively, once a regular periodic pattern has been established.

Second, in the drug-eluting contact lens case (a mode of administration currently under development for anti-VEGF drugs[10]), we consider the scenario where a series of four lenses are worn for 30 days at a time, starting on day 1, with a 1-day break between lenses, with the final 4 weeks left untreated (Fig. 5 [middle row]). This would utilize continuous wear contact lenses, which are currently in clinical use (though not of a drug-eluting type) and can be left in overnight and worn for up to a month (see, for example, www.specsavers.co.uk/contact-lenses and Lin et al.[72]). Further, Ciolino et al.[73] have demonstrated that such lenses can release drugs at a constant rate (zero-order release kinetics) for over 28 days, indicating that they could maintain a constant drug concentration in the tear film (at concentrations consistent with those used in our model), given its rapid dilution/turnover,[73] consistent with our modeling assumptions. VEGF levels were suppressed more strongly than with drops (with periodic minima of 2.17×10^{-4} and 3.25×10^{-4} pmol mL^{-1} in the aqueous and vitreous, respectively), with small transient increases in VEGF levels between lenses (with periodic maxima of 3.32×10^{-4} and 4.93×10^{-4} pmol mL^{-1} in the aqueous and vitreous, respectively). The initial minimum is achieved after about 6 days of treatment, and VEGF levels return to untreated values after about 2 weeks after treatment termination. Aqueous and vitreal ranibizumab concentrations oscillate over ranges of (7.64×10^{-2}, 0.180) and (0.111,0.183) pmol mL^{-1}, respectively, once a regular periodic pattern has been established.

Third, in the intravitreal injection case, we consider the scenario where injections are administered every 4 weeks

Investigative Ophthalmology & Visual Science

Downloaded from iovs.arvojournals.org on 09/24/2025

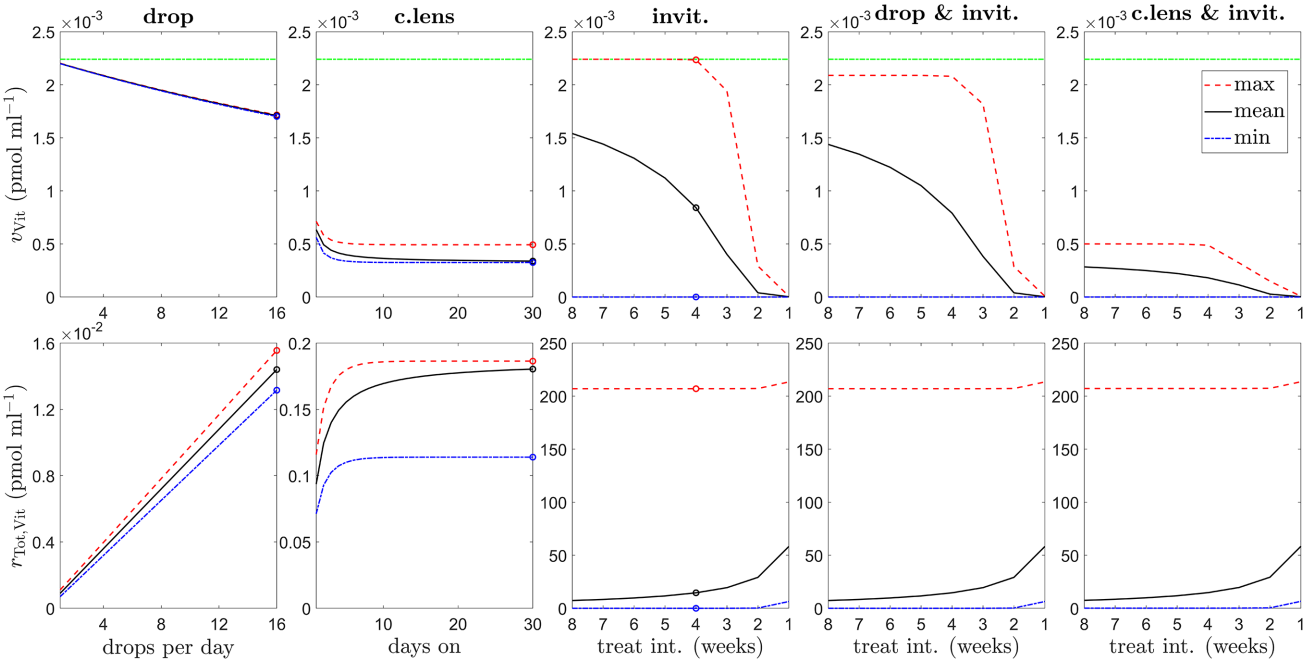

Figure 7. Effect of dosing regimen on vitreal VEGF and ranibizumab levels. Panels show variation in the maximum/mean/minimum vitreal VEGF concentration, v_{Vit} (*top row*), and maximum/mean/minimum total ranibizumab concentration, $r_{Tot,\,Vit} = r_{Vit} + u_{Vit} + 2w_{Vit}$ (*bottom row*), in response to variation in dosing frequency or duration (*first–third columns*: *circles* show the corresponding values for the dosing regimens plotted in Fig. 5). *Top row*: *horizontal green dash-dot lines* show the untreated vitreal VEGF level. *First column* (topical drops only): the number of drops per day, n_{drop}, is varied across all integer values between 1 and 16 inclusive, where the first drop of each day is administered at 0 h, with subsequent drops being administered in time increments of $16/n_{drop}$ h. Simulated for $t \in [0, 12]$ weeks, with plotted values calculated over model outputs from the interval $t \in [9, 12]$ weeks. *Second column* (drug-eluting contact lenses only): lenses are worn for n_{day} days at a time, starting on day 1, with a 1-day break between lenses, where n_{day} is varied across all integer values between 1 and 30 inclusive. Simulated for $t \in [0, 124]$ days (enough for four full treatment cycles of 31 days: 30 days on and 1 day off), with plotted values calculated over the final treatment cycle (of n_{day} days on and 1 day off). *Third column* (intravitreal injections only): the time between injections is varied across all integer values between 1 and 8 weeks inclusive, with the first injection being administered at the start of week 1. *Fourth column* (topical drops and intravitreal injections): injections are administered as in the third column, with the addition of four topical drops per day (the realistic maximum frequency[71]) at 4, 8, 12, and 16 h. *Fifth column* (drug-eluting contact lenses and intravitreal injections): injections are administered as in the third column, with the addition of drug-eluting contact lenses worn for 6 days a week (the longest duration that can be used across all interinjection intervals while allowing for a 1-day break between lenses) between days 2 and 7 of each week. *Third to fifth columns*: simulated for $t \in [0, 32]$ weeks (enough for four full treatment cycles lasting the maximum interval of 8 weeks), with plotted values calculated over model outputs from the final treatment cycle (with duration equal to the time between injections). Increasing drop or injection frequency, or increasing the time interval for which drug-eluting contact lenses are worn, increases the maximum, mean, and minimum vitreal total ranibizumab concentrations and decreases the maximum, mean, and minimum vitreal VEGF concentrations. Combining injections with drops or contact lenses visibly reduces the maximum and mean vitreal VEGF concentrations compared to injections alone, while the effect on the minimum vitreal VEGF concentration and the maximum, mean, and minimum vitreal total ranibizumab concentrations is more subtle. Equations 2–12 were solved using the default human parameters in Table 3.

(i.e., monthly, this being the highest frequency at which anti-VEGF injections are generally administered,[74,75] the aim being to show the maximum effect), at the start of weeks 1, 5, 9, and 13, with the simulation allowed to run to the end of week 16 (Fig. 5 [bottom row]). Injections reduce VEGF to by far the lowest levels (3.27×10^{-9} and 2.21×10^{-7} pmol mL^{-1} in the aqueous and vitreous, respectively), though VEGF returns to untreated values between injections. VEGF levels reach their minimum about 1.5 h after injection in the aqueous and 12 min after injection in the vitreous, and they return to untreated values after about 4 weeks after treatment termination. Aqueous and vitreal ranibizumab concentrations oscillate over ranges of (1.13×10^{-4}, 135) and (1.64×10^{-4}, 207) pmol mL^{-1} respectively.

The above results demonstrate that topical treatments have the advantage of maintaining VEGF at suppressed levels, while intravitreal treatments reduce VEGF levels far more significantly, with the disadvantage that VEGF levels return to untreated values between treatments. Therefore, we considered two further cases: dual drop/intravitreal administration and dual contact lens/intravitreal administration (see Fig. 6).

First, for dual drop/intravitreal administration, we consider the scenario where a single drop is applied at the start of hours 1 to 16 every day for the first 16 weeks, while injections are administered at the start of weeks 1, 5, 9, and 13 (Fig. 6 [top row]). The simulation runs to 20 weeks, the final 4 of which are untreated. VEGF levels remain damped between injections; aqueous and vitreal concentrations oscillating over ranges of (3.28×10^{-9}, 1.19×10^{-3}) and (2.21×10^{-7}, 1.71×10^{-3}) pmol mL^{-1}, respectively, while aqueous and vitreal ranibizumab concentrations oscillate over ranges of (8.70×10^{-3}, 135) and (1.26×10^{-2}, 207) pmol mL^{-1}, respectively.

Finally, for dual contact lens/intravitreal administration, we consider the scenario where a series of four lenses are worn for 27 days at a time, starting on day 2, with a 1-

Investigative Ophthalmology & Visual Science

Downloaded from iovs.arvojournals.org on 09/24/2025

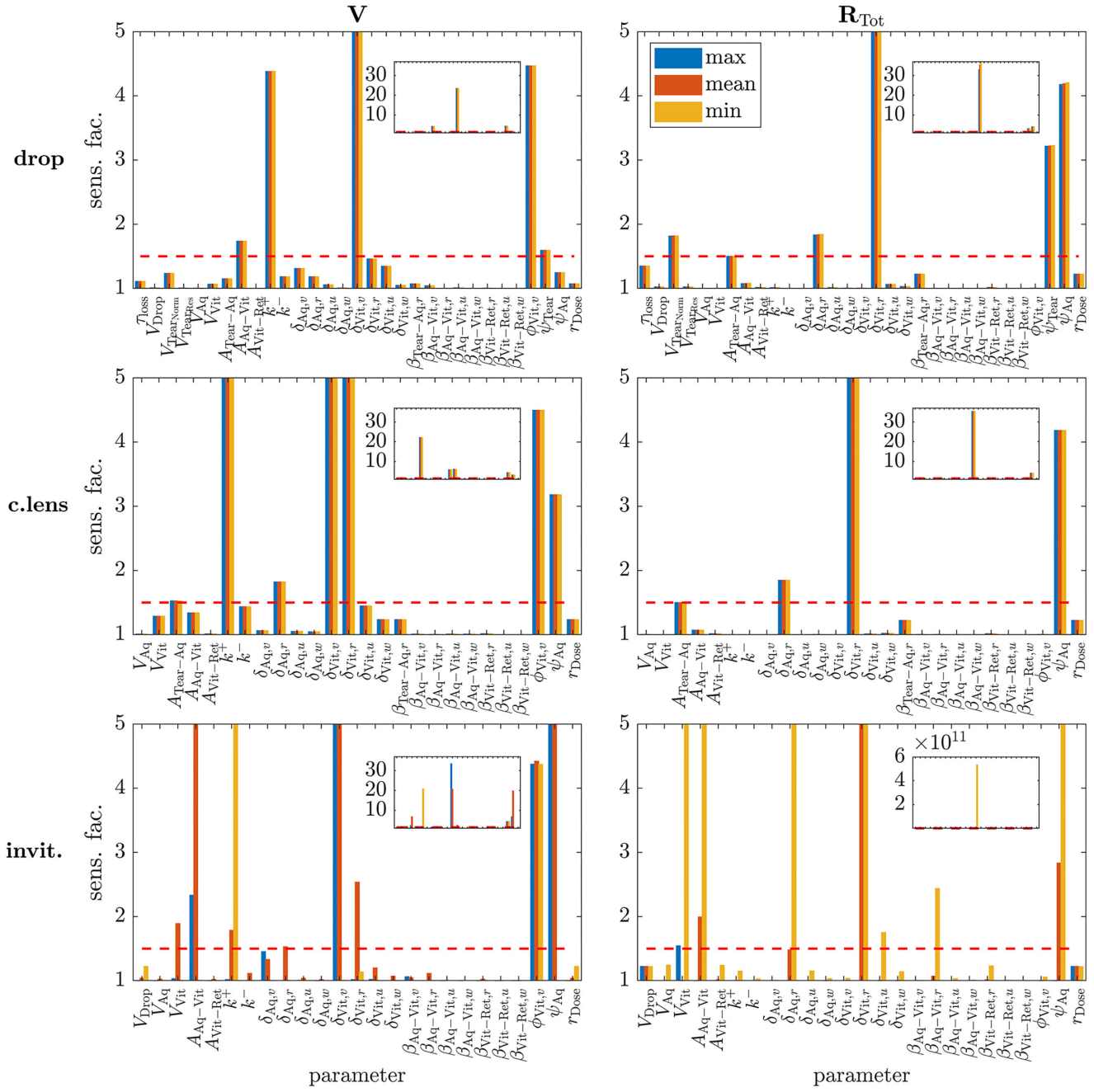

Figure 8. Local sensitivity analysis. Panels show sensitivity of the maximum/mean/minimum vitreal VEGF (V) concentration (*left column*) and total vitreal ranibizumab (R_{Tot} = R + VR + 2RVR) concentration (*right column*) to variation in model parameters over biologically realistic ranges (insets show full range of sensitivity values). Equations 2–12 were solved for $t \in [0, 12]$ weeks. *Top row*: topical drops, applied on the hour, every hour. *Middle row*: drug-eluting contact lens, worn continuously. *Bottom row*: intravitreal injections, administered at the start of weeks 1, 5, and 9. Parameters were varied individually, across 101 values uniformly distributed over the ranges given in Table 4, with the remaining parameters being held at their default values given in Table 4. For each parameter set, the maximum/mean/minimum vitreal values of V and R_{Tot} were calculated over model outputs from the interval $t \in [9, 12]$ weeks (see Supplementary Figs. S2–S7). Each sensitivity factor was then calculated as the maximum value obtained by the maximum/mean/minimum value of V or R_{Tot} over the 101 values across which the parameter was varied, divided by the corresponding minimum value over that range. The *dashed red horizontal line* demarcates the sensitivity threshold (=1.5), above which sensitivity is considered significant. The model demonstrates sensitivity to the following parameters—drops: ($V_{Tear_{Norm}}$, A_{Aq-Vit}, k^+, $\delta_{Aq,r}$, $\delta_{Vit,v}$, $\delta_{Vit,r}$, $\phi_{Vit,v}$, ψ_{Tear}, ψ_{Aq}); contact lens: ($A_{Tear-Aq}$, k^+, $\delta_{Aq,r}$, $\delta_{Vit,v}$, $\delta_{Vit,r}$, $\phi_{Vit,v}$, ψ_{Aq}), injections: (V_{Vit}, $A_{Aq\text{-}Vit}$, k^+, $\delta_{Aq,r}$, $\delta_{Vit,v}$, $\delta_{Vit,r}$, $\delta_{Vit,u}$, $\beta_{Aq\text{-}Vit,r}$, $\phi_{Vit,v}$, ψ_{Aq}).

day break between lenses, while injections are administered at the start of weeks 1, 5, 9, and 13 (on the days without contact lenses; Fig. 6 [bottom row]). The simulation runs to 20 weeks, the final 4 of which are untreated. VEGF levels are damped more strongly than with drops between injections, with aqueous and vitreal concentrations oscillating over ranges of (3.29×10^{-9}, 2.17×10^{-4}) and (2.20×10^{-7}, 3.25×10^{-4}) pmol mL^{-1}, respectively, while aqueous and

Investigative Ophthalmology & Visual Science

Downloaded from iovs.arvojournals.org on 09/24/2025

vitreal ranibizumab concentrations oscillate over ranges of (0.180,135) and (0.183,207) pmol mL^{-1}, respectively.

Dosing Regimens. Having explored the effects of specific treatment regimens in Figures 5 and 6, we considered the effect of varying the dosing frequency or duration for single and dual modes of administration (see Fig. 7).

For a single mode of administration (Fig. 7 [columns 1–3]—see figure legend for detailed descriptions of each regimen), it was found that increasing topical drop or intravitreal injection frequency, or increasing the time interval for which drug-eluting contact lenses are worn, increases the maximum, mean, and minimum vitreal total ranibizumab concentrations ($r_{\text{Tot, Vit}} = r_{\text{Vit}} + u_{\text{Vit}} + 2w_{\text{Vit}}$) and decreases the maximum, mean, and minimum vitreal VEGF concentrations (v_{Vit}). Drops have the weakest effect and injections the strongest effect on minimal vitreal VEGF levels, the effect of contact lenses being intermediate between the two. With regard to the range between minimum and maximum vitreal VEGF levels, this is widest for injections and narrowest for drops, with contact lenses having an intermediate range. The maximum vitreal VEGF concentration returns to untreated levels for interinjection intervals of 4 weeks or longer.

Combining injections with drops or contact lenses visibly reduces the maximum and mean vitreal VEGF concentrations compared to injections alone, while the effect on the minimum vitreal VEGF concentration (and on the maximum, mean, and minimum vitreal total ranibizumab concentrations) is relatively subtle (Fig. 7 [columns 4–5]—see figure legend for detailed descriptions of each regimen). Of greatest significance, the addition of drops or contact lenses prevents vitreal VEGF levels from returning to untreated levels (for interinjection intervals of 4 weeks or longer).

Sensitivity Analysis. A local sensitivity analysis was performed to determine the effect of varying each parameter upon key model outputs (see Methods—Sensitivity Analysis for details). Each mode of administration was considered in isolation: topical drops, applied on the hour, every hour (Fig. 8 [top row]); a drug-eluting contact lens, worn continuously (Fig. 8 [middle row]); and intravitreal injections, administered at the start of weeks 1, 5, and 9 (Fig. 8 [bottom row]). (While, in practice, drops would not be administered every hour of the day, and a continuous wear contact lens could be worn for a maximum of 30 days, this is not important for the purposes of our sensitivity analysis.) For topical drops, the model demonstrates sensitivity to ($V_{\text{Tear}_{\text{Norm}}}$, $A_{\text{Aq-Vit}}$, k^+, $\delta_{\text{Aq},r}$, $\delta_{\text{Vit},v}$, $\delta_{\text{Vit},r}$, $\phi_{\text{Vit},v}$, ψ_{Tear}, ψ_{Aq}); for a drug-eluting contact lens, the model demonstrates sensitivity to ($A_{\text{Tear-Aq}}$, k^+, $\delta_{\text{Aq},r}$, $\delta_{\text{Vit},v}$, $\delta_{\text{Vit},r}$, $\phi_{\text{Vit},v}$, ψ_{Aq}); and for intravitreal injections, the model demonstrates sensitivity to (V_{Vit}, $A_{\text{Aq-Vit}}$, k^+, $\delta_{\text{Aq},r}$, $\delta_{\text{Vit},v}$, $\delta_{\text{Vit},r}$, $\delta_{\text{Vit},u}$, $\beta_{\text{Aq-Vit},r}$, $\phi_{\text{Vit},v}$, ψ_{Aq}). See Supplementary Figs. S2–S7 for detailed plots showing the variation of each key output with each parameter under each mode of administration.

Discussion

Topical application of anti-VEGF drugs provides a promising alternative or addition to intravitreal injections, which are expensive, uncomfortable, and risk infection. In this study, we took a combined experimental-modeling approach to investigate the potential for topical ranibizumab administration in the treatment of wet AMD, providing deeper insights than would be possible by employing either approach in isolation. Our experimental results and modeling predictions suggest that topical application may be a promising means of ranibizumab administration, either in isolation or in combination with intravitreal injections, reducing peak vitreal VEGF levels and thereby potentially reducing the frequency of injections and improving overall treatment efficacy. While formulated with ranibizumab in mind, our model could easily be adapted to simulate topical and intravitreal administration of other anti-VEFG drugs (such as bevacizumab and aflibercept), and of ocular drugs in general, including new and upcoming treatments for non-neovascular AMD such as pegcetacoplan and avacincaptad pegol.[76–78] Using our mathematical model and variations upon it, we can accelerate the development of new drugs, administration techniques, and regimens, testing a range of scenarios quickly and at low cost, as well as reducing, replacing, and refining animal experiments.

Our experiments in ex vivo porcine eyes revealed that our (polyarginine-based) CPP allows topical ranibizumab to penetrate the cornea (in agreement with de Cogan et al.[9]), though it reduces ranibizumab's efficacy in neutralizing VEGF for intravitreal treatment. This latter effect is likely due to CPP reducing ranibizumab's ability to bind to VEGF in the time interval, postadministration, during which CPPs unbind from ranibizumab. As would be expected, intravitreal ranibizumab treatments result in higher vitreal ranibizumab levels and more rapid and complete reduction of vitreal VEGF than topical treatment.

Mathematical modeling allowed us both to gain a deeper insight into our experimental results and to extrapolate to the living human eye. Fitting our model to the experimental data, we determined the permeabilities of the porcine cornea and suspensory ligaments (zonule) to ranibizumab, VEGF, and their compounds (RV and RVR), extrapolating these values for humans. Further, our model fits suggest that a substantive proportion of the drop volume remains on the eye during experiments, consistent with visual observations.

In the in vivo human eye, we used our mathematical model to simulate ranibizumab and VEGF levels (and those of their compounds) in the tear film, aqueous, and vitreous, under a number of different treatment regimens. We note that, given our model does not contain retinal or choroidal compartments, the best measure of each treatment's efficacy is its effect on vitreal VEGF levels. First, we considered cases where treatment is applied via a single mode of administration: drops, drug-eluting contact lenses, or intravitreal injections. We found that topical therapies (drops and contact lenses) maintain suppressed vitreal VEGF levels (and maintain vitreal ranibizumab levels), drug-eluting contact lenses having a stronger suppressive effect given that they maintain a constant supply of ranibizumab to the tear film, and ranibizumab delivered via drops is quickly diluted and removed from the tear. By comparison, intravitreal injections suppress vitreal VEGF levels more strongly, as would be expected given that a large ranibizumab dose is delivered directly to the vitreous; however, the effect wears off between treatments, with vitreal VEGF levels returning to untreated values between treatments for interinjection intervals of 4 weeks or greater. This is on the lower end of the range of VEGF suppression periods (26–69 days) measured in humans following an intravitreal ranibizumab injection.[79]

If topical treatment were able to maintain vitreal (and, hence, retinal/choroidal) VEGF levels at sufficiently low concentrations, then topical therapy could replace intravitreal therapy. Even if this is not possible, topical modes of administration could potentially be used in combination with intravitreal treatments, increasing the overall efficacy of the treatment and reducing the frequency with

Investigative Ophthalmology & Visual Science

Downloaded from iovs.arvojournals.org on 09/24/2025

which intravitreal injections need to be administered. To this end, we simulated dual topical and intravitreal administration, combining either drops and injections or drug-eluting contact lenses and injections. Our simulations suggest that dual therapies would provide the best of both worlds, with injections providing highly suppressed vitreal VEGF levels and topical treatment preventing VEGF levels from returning to untreated values between injections (such that VEGF levels do not exceed the suppressed levels achieved by applying topical treatment alone).

Local sensitivity analysis revealed the parameters to which the vitreal ranibizumab and VEGF concentrations are most sensitive. Some of these parameters, namely $V_{\text{Tear}_{\text{Norm}}}$, V_{Vit}, $A_{\text{Tear-Aq}}$, $A_{\text{Aq-Vit}}$, $\delta_{\text{Vit},v}$, $\delta_{\text{Vit},u}$, $\phi_{\text{Vit},v}$, and ψ_{Aq}, may vary between patients, though they are not factors that we could realistically alter, being fundamental to the eye's geometry, biochemistry, or biomechanics. However, other parameters, namely k^+, $\delta_{\text{Aq},r}$, $\delta_{\text{Vit},r}$, $\beta_{\text{Aq-Vit},r}$, and ψ_{Tear}, could potentially be modified by redesigning the drug or mode of application. For example, k^+ could perhaps be increased, and $\beta_{\text{Aq-Vit},r}$ (for intravitreal delivery), $\delta_{\text{Aq},r}$ and $\delta_{\text{Vit},r}$ decreased, by altering the drug's molecular structure, while ψ_{Tear} could be decreased by increasing ranibizumab's residence time in the tear film, for example, using a molecular anchor such as collagen binding domains[80] or wheat germ agglutinin,[81] or viscosity increasing polymers such as polyacrylates and polyvinyl alcohols.[41]

This study has a number of limitations. To begin, there were several experimental limitations. First, VEGF was not detected in vitreal controls. The reason for this is unclear; however, it has previously been shown that VEGF is frequently undetectable in the vitreous of healthy eyes.[82] Second, ranibizumab in the aqueous was outside the limits of detection at 1 h for topical treatment with ranibizumab and CPP, despite being detected at all other time points. The reason for this anomaly is unclear; however, we are confident in the other aqueous ranibizumab measurements given they are well above the control value (0 pmol mL^{-1}) and show a clear, statistically significant, increasing trend, coincident with a significant drop in aqueous VEGF levels. Third, good mathematical model fits to the ex vivo porcine ranibizumab measurements were achieved in all cases, except in the vitreous compartment for topical treatment with CPP. This is most likely because the measured ranibizumab levels in the vitreal compartment are inaccurate, given that they are within the levels of the control measurements, which were themselves nonzero, likely due to the effects of vitreal proteins being mis-detected as ranibizumab. Fourth, measured vitreal ranibizumab values following intravitreal ranibizumab injections (with and without CPP) were much lower than would be expected based on the injected dose concentration (and volume). This is most likely because, despite being placed on a shaker, vitreal ranibizumab does not spread out uniformly from the injection site over the time frame of our experiments, and our samples were taken from a portion of the vitreous away from the injection site (see also the discussion of the well-mixed assumption below). When fitting our model to the intravitreal ranibizumab treatment without CPP data to find the permeability of the aqueous-vitreous interface, we initialized the simulation using the measured intravitreal ranibizumab concentration, since this value is more representative of the vitreal ranibizumab concentration near the aqueous-vitreous interface (away from the injection site) than a value that assumes a uniform distribution. This resulted in a similar permeability value to that obtained by fitting to the topical treatment data.

There are also limitations concerning drug delivery. First, since the aim of this article was not to optimize drug delivery systems, we did not explore the thermocalorimetric properties of CPP-ranibizumab formulations. Second, since the aim of this article was not to develop a novel delivery system, we did not explore how CPP would enhance retinal bioavailability of biologics compared to other carriers, such as nanostructured lipid carriers and annexin A5.[83,84] Third, we have not considered how favorable the physicochemical properties of ranibizumab are for CPP delivery, compared to other anti-VEGF drugs.[85] In the present study, we used ranibizumab as a proof of concept based on previously published data,[9] noting that while ranibizumab is negatively charged, it does not have a strong negative charge compared to aflibercept and bevacizumab, and that CPPs can facilitate permeation beyond their ability to complex.

There is a potential limitation in extrapolating corneal and suspensory ligament permeability values from ex vivo pig eyes to in vivo human eyes. While the pig eyes are ex vivo, they are fresh, having been taken within hours of the animal being killed. Therefore, we would not expect this to significantly alter the permeabilities from what they would have been in vivo.[86–88] Regarding extrapolating between species, the structure of the cornea and suspensory ligaments are the same in porcine and human eyes, while, as described in Appendix A: Parameter Justification, we account for the difference in corneal thickness between porcine and human eyes by making an appropriate scaling to the permeability value. We also account for the difference in surface area between the porcine and human cornea and suspensory ligaments through using appropriate values for $A_{\text{Tear-Aq}}$ and $A_{\text{Aq-Vit}}$ in each species.

Another limitation concerns our modeling assumption that CPPs only aid the passage of ranibizumab from the tear film to the aqueous and not across the aqueous-vitreous or vitreo-retinal interfaces. In the scenario that CPPs act by binding to ranibizumab to chaperone it across barriers (a binding interaction being suggested by our experiments described in the Methods—Experimental Methods—Zeta Potential section), this assumes that unbinding of ranibizumab and CPP molecules dominates over binding of these molecules in the larger volume and hence more diluted environments of the aqueous and vitreous (as compared to the tear film). In the scenario that CPPs act directly on barriers to increase their permeability, without directly interacting with ranibizumab, this assumes that the dilution of CPPs in the aqueous and vitreous will severely limit their effects on barrier permeability. Current evidence suggests that the binding of CPPs does not inhibit the interaction of ranibizumab with VEGF,[32] and given our argument above, it is likely that ranibizumab is mostly unbound from CPPs in the aqueous and vitreous following topical treatment (though our experiments suggest that CPP may reduce ranibizumab's interaction with VEGF for the first few hours after intravitreal injections of ranibizumab with CPPs, this effect being insignificant in the long-term given that the time interval between intravitreal injections is typically on the order of weeks). Future mathematical models could include separate variables for the concentrations of CPP and CPP-ranibizumab compounds in the tear, aqueous, and vitreal compartments, exploring their interactions and effects in greater detail.

A further limitation concerns our well-mixed assumption. In using an ODE model (a well-established approach for modeling ocular drug delivery[17–19]), we have limited our spatial representation to compartmentalization, while

Investigative Ophthalmology & Visual Science

Downloaded from iovs.arvojournals.org on 09/24/2025

making the simplifying assumption that species are well-mixed within compartments. In reality, chemical species would be spatially distributed within ocular compartments and subject to processes such as advection and diffusion, which cannot be captured by an ODE model. We argue that the well-mixed assumption is justified in the tear film and aqueous, given their low volume and the mixing effect of the fluid flow within them. Simulation studies for the aged, and hence liquefied or partially liquefied vitreous (relevant to the aged AMD eyes considered in this study), predict that drug transport will occur on a time scale of seconds to hours.[21–23,26] This is fast enough to justify the well-mixed assumption for our human simulations that occur over a period of several weeks, though it suggests that full mixing may not have occurred within the shorter time frame of our experiments and their simulations, despite placing eyes on a shaker to approximate saccadic/translational motion and promote mixing. Views vary as to the importance of the position of the intravitreal source/injection site, with some finding that it does not have a large impact on drug distribution, at least after the first few seconds,[21,23] while others suggest that it is likely to have a large impact on the spatial distribution of drug uptake by the retina.[22] Of relevance to topical delivery, Balachandran and Barocas[21] considered transscleral drug delivery (for which the drug also enters the vitreous through its perimeter), with drug transport on a time scale of minutes to hours, with the position of the source having little impact on drug distribution.

In future studies, we will extend this work on both experimental and mathematical fronts. Future experimental work could include measuring retinal ranibizumab and VEFG concentrations in addition to those in the aqueous and vitreous, measuring CPP concentrations in each compartment, making more frequent measurements over a larger time span with more repeats, and measurements using in vivo animal eyes in which key elements such as clearance mechanisms and VEGF production are active. Preferably, this would be done in eyes of a similar size to human eyes such as porcine eyes, though rat eyes would also be informative. It would also be interesting to repeat these measurements with drug-eluting contact lenses and to explore ways to further improve ranibizumab's corneal penetration and tear residence time, as well as their effect on treatment efficacy. Future mathematical modeling will include extending our ODE model to include a retinal compartment (in a similar way to Hutton-Smith et al.[19]) and developing a spatially resolved partial differential equation model accounting for both the advective and diffusive transport of ranibizumab, VEGF, and their compounds.

Acknowledgments

This study was funded through the Centre for Systems Modeling and Quantitative Biomedicine by the University of Birmingham Dynamic Investment Fund. P.A.R. was funded by the University of Birmingham Dynamic Investment Fund. C.N.T. was funded by Fight for Sight. G.B.P. was funded by the Kennedy Trust for Rheumatology Research. J.A.R. was funded by the Macular Society. L.J.H. was funded in part by the NIHR Birmingham Biomedical Research Centre and a Medical Research Council Impact Acceleration Account (MR/X502996/1).

Disclosure: **P.A. Roberts**, None; **C.N. Thomas**, None; **G. Bellamy Plaice**, None; **J.A. Roberts**, None; **M.-C. Jones**, None; **J.W. Andrews**, None; **L.J. Hill**, None

References

1. Wong WL, Su X, Li X, et al. Global prevalence of age-related macular degeneration and disease burden projection for 2020 and 2040: a systematic review and meta-analysis. *Lancet Glob Health*. 2024;2(2):e106–e116.
2. Ferris FL, Wilkinson CP, Bird A, et al. Clinical classification of age-related macular degeneration. *Ophthalmology*. 2013;120(4):844–851.
3. Coleman HR, Chan CC, Ferris FL, III, Chew EY. Age-related macular degeneration. *Lancet*. 2008;372(9652):1835–1845.
4. Jager RD, Mieler WF, Miller JW. Age-related macular degeneration. *N Engl J Med*. 2008;358(24):2606–2617.
5. Yeo NJY, Chan EJJ, Cheung C. Choroidal neovascularization: mechanisms of endothelial dysfunction. *Front Pharmacol*. 2019;10:1363.
6. García-Quintanilla L, Luaces-Rodríguez A, Gil-Martínez M, et al. Pharmacokinetics of intravitreal anti-VEGF drugs in age-related macular degeneration. *Pharmaceutics*. 2019;11(8):365.
7. Ghasemi Falavarjani K, Nguyen QD. Adverse events and complications associated with intravitreal injection of anti-VEGF agents: a review of literature. *Eye*. 2013;27(7):787–794.
8. Gadziński P, Froelich A, Wojtyłko M, Białek A, Krysztofiak J, Osmałek T. Microneedle-based ocular drug delivery systems - recent advances and challenges. *Beilstein J Nanotechnol*. 2022;13:1167–1184.
9. de Cogan F, Hill LJ, Lynch A, et al. Topical delivery of anti-VEGF drugs to the ocular posterior segment using cell-penetrating peptides. *Invest Ophthalmol Vis Sci*. 2017;58(5):2578–2590.
10. Ross AE, Bengani LC, Tulsan R, et al. Topical sustained drug delivery to the retina with a drug-eluting contact lens. *Biomaterials*. 2019;217:119285.
11. Löscher M, Seiz C, Hurst J, Schnichels S. Topical drug delivery to the posterior segment of the eye. *Pharmaceutics*. 2022;14(1):134.
12. Derossi D, Calvet S, Trembleau A, Brunissen A, Chassaing G, Prochiantz A. Cell internalization of the third helix of the antennapedia homeodomain is receptor-independent. *J Biol Chem*. 1996;271(30):18188–18193.
13. Suzuki T, Futaki S, Niwa M, Tanaka S, Ueda K, Sugiura Y. Possible existence of common internalization mechanisms among arginine-rich peptides. *J Biol Chem*. 2002;277(4):2437–2443.
14. Johnson LN, Cashman SM, Kumar-Singh R. Cell-penetrating peptide for enhanced delivery of nucleic acids and drugs to ocular tissues including retina and cornea. *Mol Ther*. 2008;16(1):107–114.
15. Rothbard JB, Garlington S, Lin Q, et al. Conjugation of arginine oligomers to cyclosporin A facilitates topical delivery and inhibition of inflammation. *Nat Med*. 2000;6(11):1253–1257.
16. Vivès E, Brodin P, Lebleu B. A truncated HIV-1 tat protein basic domain rapidly translocates through the plasma membrane and accumulates in the cell nucleus. *J Biol Chem*. 1997;272(25):16010–16017.
17. Hutton-Smith LA, Gaffney EA, Byrne HM, Maini PK, Schwab D, Mazer NA. A mechanistic model of the intravitreal pharmacokinetics of large molecules and the pharmacodynamic suppression of ocular vascular endothelial growth factor levels by ranibizumab in patients with neovascular age-related macular degeneration. *Mol Pharm*. 2016;13(9):2941–2950.

Investigative Ophthalmology & Visual Science

Downloaded from iovs.arvojournals.org on 09/24/2025

18. Hutton-Smith LA, Gaffney EA, Byrne HM, Maini PK, Gadkar K, Mazer NA. Ocular pharmacokinetics of therapeutic antibodies given by intravitreal injection: estimation of retinal permeabilities using a 3-compartment semi-mechanistic model. *Mol Pharm.* 2017;14(8):2690–2696.
19. Hutton-Smith LA, Gaffney EA, Byrne HM, Caruso A, Maini PK, Mazer NA. Theoretical insights into the retinal dynamics of vascular endothelial growth factor in patients treated with ranibizumab, based on an ocular pharmacokinetic/pharmacodynamic model. *Mol Pharm.* 2018;15(7):2770–2784.
20. Toffoletto N, Saramago B, Serro AP, Chauhan A. A physiology-based mathematical model to understand drug delivery from contact lenses to the back of the eye. *Pharm Res.* 2023;40(8):1939–1951.
21. Balachandran RK, Barocas VH. Contribution of saccadic motion to intravitreal drug transport: theoretical analysis. *Pharm Res.* 2011;28(5):1049–1064.
22. Bonfiglio A, Repetto R, Siggers JH, Stocchino A. Investigation of the motion of a viscous fluid in the vitreous cavity induced by eye rotations and implications for drug delivery. *Phys Med Biol.* 2013;58(6):1969–1982.
23. Ferroni M, De Gaetano F, Cereda MG, Boschetti F. A drug delivery analysis of large molecules in ocular vitreous chamber: dependency on saccadic movements after intravitreal injection. *Med Eng Phys.* 2020;82:49–57.
24. Missel PJ. Simulating intravitreal injections in anatomically accurate models for rabbit, monkey, and human eyes. *Pharm Res.* 2012;29(12):3251–3272.
25. Ruffni A, Casalucci A, Cara C, Ethier CR, Repetto R. Drug distribution after intravitreal injection: a mathematical model. *Invest Ophthalmol Vis Sci.* 2024;65(4):9.
26. Stocchino A, Repetto R, Siggers JH. Mixing processes in the vitreous chamber induced by eye rotations. *Phys Med Biol.* 2010;55(2):453–467.
27. Bhandari A. Ocular fluid mechanics and drug delivery: a review of mathematical and computational models. *Pharm Res.* 2021;38(12):2003–2033.
28. del Amo EM, Rimpelä A-K, Heikkinen E, et al. Pharmacokinetic aspects of retinal drug delivery. *Prog Retin Eye Res.* 2017;57:134–185.
29. Hernandez RJ, Roberts PA, El-Bouri WK. Advancing treatment of retinal disease through in silico trials. *Prog Biomed Eng.* 2023;5(2):022002.
30. Sadeghi A, Subrizi A, del Amo EM, Urtti A. Mathematical models of ocular drug delivery. *Invest Ophthalmol Vis Sci.* 2024;65(11):28.
31. Roberts PA, Gaffney EA, Luthert PJ, Foss AJE, Byrne HM. Mathematical and computational models of the retina in health, development and disease. *Prog Retin Eye Res.* 2016;53:48–69.
32. Hu W, Cai W, Wu Y, et al. Topical application of cellpenetrating peptide modified anti-VEGF drug alleviated choroidal neovascularization in mice. *Int J Nanomed.* 2024;19:35–51.
33. Ferrara N. Vascular endothelial growth factor and age-related macular degeneration: from basic science to therapy. *Nat Med.* 2010;16(10):1107–1111.
34. Ang WJ, Zunaina E, Norfadzillah AJ, et al. Evaluation of vascular endothelial growth factor levels in tears and serum among diabetic patients. *PLoS One.* 2019;14(8):1–12.
35. Rentka A, Hársfalvi J, Berta A, et al. Vascular endothelial growth factor in tear samples of patients with systemic sclerosis. *Mediators Inflamm.* 2015;2015(1):573681.
36. Shahidatul-Adha M, Zunaina E, Aini-Amalina MN. Evaluation of vascular endothelial growth factor (VEGF) level in the tears and serum of age-related macular degeneration patients. *Sci Rep.* 2022;12(1):4423.
37. Murray JD. *Mathematical Biology: I. An Introduction* (3rd ed.). New York, NY: Springer; 2002.
38. Smith DW, Lee C-J, Gardiner BS. No flow through the vitreous humor: how strong is the evidence? *Prog Retin Eye Res.* 2020;78:100845.
39. Brar VS, Sen HN, American Academy of Ophthalmology,Law SK, et al. 2020-2021 Basic and Clinical Science Course(tm) (BCSC), Section 02: fundamentals and Principles of Ophthalmology. *Basic and Clinical Science Course*. American Academy of Ophthalmology; 2020, https://store.aao.org/basic-and-clinical-science-course-section-02-fundamentals-and-principles-of-ophthalmology.html.
40. Gaudana R, Ananthula HK, Parenky A, K.Mitra A. Ocular drug delivery. *AAPS J.* 2010;12(3):348–360.
41. Grassiri B, Zambito Y, Bernkop-Schnürch A. Strategies to prolong the residence time of drug delivery systems on ocular surface. *Adv Colloid Interface Sci.* 2021;288:102342.
42. Mofidfar M, Abdi B, Ahadian S, et al. Drug delivery to the anterior segment of the eye: a review of current and future treatment strategies. *Int J Pharm.* 2021;607:120924.
43. Subrizi A, del Amo EM, Korzhikov-Vlakh V, Tennikova T, Ruponen M, Urtti A. Design principles of ocular drug delivery systems: importance of drug payload, release rate, and material properties. *Drug Discov Today.* 2019;24(8):1446–1457.
44. Mishima S, Gasset A, Klyce SD, Jr, Baum JL. Determination of tear volume and tear flow. *Invest Ophthalmol Vis Sci.* 1966;5(3):264–276.
45. Scherz W, Doane MG, Dohlman CH. Tear volume in normal eyes and keratoconjunctivitissicca. *Albrecht von Graefes Arch Klin Ophthal.* 1974;192(2):141–150.
46. Agrahari V, Mandal A, Agrahari V, et al. A comprehensive insight on ocular pharmacokinetics. *Drug Deliv Transl Res.* 2016;6(6):735–754.
47. Mishima S. Clinical pharmacokinetics of the eye. Proctor lecture. *Invest Ophthalmol Vis Sci.* 1981;21(4):504–541.
48. Toris CB, Yablonski ME, Wang Y-L, Camras CB. Aqueous humor dynamics in the aging human eye. *Am J Ophthalmol.* 1999;127(4):407–412.
49. Shrader SM, Greentree WF. Göttingen minipigs in ocular research. *Toxicol Pathol.* 2018;46(4):403–407.
50. Vézina M. Assessing ocular toxicology in laboratory animals. In: Weir AB, Collins M, eds. *Molecular and Integrative Toxicology, chapter Comparative Ocular Anatomy in Commonly Used Laboratory Animals*. Totowa, NJ: Humana Press; 2012.
51. Krohne TU, Eter N, Holz FG, Meyer C. Intraocular pharmacokinetics of bevacizumab after a single intravitreal injection in humans. *Am J Ophthalmol.* 2008;146(4):508–512.
52. Zhu Q, Ziemssen F, Henke-Fahle S, et al. Vitreous levels of bevacizumab and vascular endothelial growth factor-A in patients with choroidal neovascularization. *Ophthalmology.* 2008;115(10):1750–1755.e1.
53. Altman PL. *Blood and Other Body Fluids. Biological Handbooks*. Washington, D. C.: Federation of American Societies for Experimental Biology; 1961.
54. Shafiee A, McIntire GL, Sidebotham LC, Ward KW. Experimental determination and allometric prediction of vitreous volume, and retina and lens weights in Göttingen minipigs. *Vet Ophthalmol.* 2008;11(3):193–196.
55. Bron AJ, Tripathi RC, Tripathi BJ. *Wolff's Anatomy of the Eye and Orbit*. 8th ed. London: Chapman & Hall Medical; 1997.
56. Rüfer F, Schröder A, Erb C. White-to-white corneal diameter: normal values in healthy humans obtained with the orbscan II topography system. *Cornea.* 2005;24(3):259–261.

Investigative Ophthalmology & Visual Science

Downloaded from iovs.arvojournals.org on 09/24/2025

57. Olsen TW, Sanderson S, Feng X, Hubbard WC. Porcine sclera: thickness and surface area. *Invest Ophthalmol Vis Sci.* 2002;43(8):2529–2532.
58. F.Manns J-MP, Denham D, Billotte C, et al. Optomechanical response of human and monkey lenses in a lens stretcher. *Invest Ophthalmol Vis Sci.* 2007;48(7):3260–3268.
59. Asejczyk-Widlicka M, Schachar R, Pierscionek BK. Optical coherence tomography measurements of the fresh porcine eye and response of the outer coats of the eye to volume increase. *J Biomed Opt.* 2008;13(2):024002.
60. Bartholomew LR, Pang DX, Sam DA, Cavender JC. Ultrasound biomicroscopy of globes from young adult pigs. *Am J Vet Res.* 1997;58(9):942–948.
61. Hahn J, Fromm M, Halabi FAL, et al. Measurement of ex vivo porcine lens shape during simulated accommodation, before and after fs-laser treatment. *Invest Ophthalmol Vis Sci.* 2015;56(9):5332–5343.
62. Reilly MA, Hamilton PD, Perry G, Ravi N. Comparison of the behavior of natural and refilled porcine lenses in a robotic lens stretcher. *Exp Eye Res.* 2009;88(3):483–494.
63. Sanchez I, R.Martin FU, Fernandez-Bueno I. The parameters of the porcine eyeball. *Graefes Arch Clin Exp Ophthal.* 2011;249(4):475–482.
64. Watson R, Gray W, Sponsel WE, et al. Simulations of porcine eye exposure to primary blast insult. *Transl Vis Sci Technol.* 2015;4(4):8.
65. Webvision, http://webvision.med.utah.edu/. Accessed May 28, 2024.
66. Papadopoulos N, Martin J, Ruan Q, et al. Binding and neutralization of vascular endothelial growth factor (VEGF) and related ligands by VEGF trap, ranibizumab and bevacizumab. *Angiogenesis.* 2012;15(2):171–185.
67. Ferrara N, Damico L, Shams N, Lowman H, Robert K. Development of ranibizumab, an antivascular endothelial growth factor antigen binding fragment, as therapy for neovascular age-related macular degeneration. *Retina.* 2006;26(8):859–870.
68. Penn JS, Madan A, Caldwell RB, Bartoli M, Caldwell RW, Hartnett ME. Vascular endothelial growth factor in eye disease. *Prog Retin Eye Res.* 2008;27(4):331–371.
69. McLaren JW. Measurement of aqueous humor flow. *Exp Eye Res.* 2009;88(4):641–647.
70. Tasman W, Jaeger EA. *Duane's Ophthalmology*. Philadelphia: Lippincott Williams & Wilkins (LWW); 2013.
71. Samoilă L, Vos¸tinaru O, Dinte E, et al. Topical treatment for retinal degenerative pathologies: a systematic review. *Int J Mol Sci.* 2023;24(9):8045.
72. Lin MC, Yeh TN, Graham AD, et al. Ocular surface health during 30-day continuous wear: rigid gas-permeable versus silicone hydrogel hyper-O2 transmitted contact lenses. *Invest Ophthalmol Vis Sci.* 2011;52(6):3530–3538.
73. Ciolino JB, Hoare TR, Iwata NG, et al. A drug-eluting contact lens. *Invest Ophthalmol Vis Sci.* 2009;50(7):3346–3352.
74. Reitan G, Kjellevold Haugen IB, Andersen K, Bragadottir R, Bindesbøll C. Through the eyes of patients: understanding treatment burden of intravitreal anti-VEGF injections for nAMD patients in Norway. *Clin Ophthalmol.* 2023;17:1465–1474.
75. Wecker T, Grundel B, Reichl S, et al. Anti-VEGF injection frequency correlates with visual acuity outcomes in pro re nata neovascular AMD treatment. *Sci Rep.* 2019;9(1):3301.
76. Chew EY. Complement inhibitors for the treatment of geographic atrophy. *Lancet.* 2023;402(10411):1396–1398.
77. Heier JS, Lad EM, Holz FG, et al. Pegcetacoplan for the treatment of geographic atrophy secondary to age-related macular degeneration (OAKS and DERBY): two multicentre, randomised, double-masked, sham-controlled, phase 3 trials. *Lancet.* 2023;402(10411):1434–1448.
78. Khanani AM, Patel SS, Staurenghi G, et al. Efficacy and safety of avacincaptad pegol in patients with geographic atrophy (GATHER2): 12-month results from a randomised, double-masked, phase 3 trial. *Lancet.* 2023;402(10411):1449–1458.
79. Muether PS, Hermann MM, Dröge K, Kirchhof B, Fauser S. Long-term stability of vascular endothelial growth factor suppression time under ranibizumab treatment in age-related macular degeneration. *Am J Ophthalmol.* 2013;156(5):989–993.e2.
80. Klarlund JK, Callaghan JD, Stella NA, Kowalski RP, McNamara NA, Shanks RMQ. Use of collagen binding domains to deliver molecules to the cornea. *J Ocul Pharmacol Ther.* 2019;35(9):491–496.
81. Klarlund J, Romanowski EG, Romanowski J, Davoli K, McNamara NA, Shanks RMQ. Overcoming washout of biologics after topical application to the ocular surface. *Invest Ophthalmol Vis Sci.* 2023;64(8):5134.
82. Aiello LP, Avery RL, Arrigg PG, et al. Vascular endothelial growth factor in ocular fluid of patients with diabetic retinopathy and other retinal disorders. *N Engl J Med.* 1994;331(22):1480–1487.
83. Davis BM, Normando EM, Guo L, et al. Topical delivery of avastin to the posterior segment of the eye in vivo using annexin A5-associated liposomes. *Small.* 2014;10(8):1575–1584.
84. Platania CBM, Cas MD, Cianciolo S, et al. Novel ophthalmic formulation of myriocin: implications in retinitis pigmentosa. *Drug Deliv.* 2019;26(1):237–243.
85. Platania CBM, Di Paola L, Leggio GM, et al. Molecular features of interaction between VEGFA and anti-angiogenic drugs used in retinal diseases: a computational approach. *Front Pharmacol.* 2015;6(248), https://doi.org/10.3389/fphar.2015.00248.
86. Grass GM, Robinson JR. Mechanisms of corneal drug penetration I: in vivo and in vitro kinetics. *J Pharm Sci.* 1988;77(1):3–14.
87. Santana CP, Matter B, Patil MA, Silva-Cunha A, Kompella UB. Corneal permeability and uptake of twenty-five drugs: species comparison and quantitative structure-permeability relationships. *Pharmaceutics.* 2023;15(6):1646.
88. Watsky MA, McDermott ML, Edelhauser HF. In vitro corneal endothelial permeability in rabbit and human: the effects of age, cataract surgery and diabetes. *Exp Eye Res.* 1989;49(5):751–767.
89. Chang AY, Purt B. Biochemistry, tear film, 2024, https://pubmed.ncbi.nlm.nih.gov/34283502/.
90. Djebli N, Khier S, Griguer F, et al. Ocular drug distribution after topical administration: population pharmacokinetic model in rabbits. *Eur J Drug Metab Pharmacokinet.* 2017;42(1):59–68.
91. Van Haeringen NJ. Clinical biochemistry of tears. *Surv Ophthalmol.* 1981;26(2):84–96.
92. Fontana ST, Brubaker RF. Volume and depth of the anterior chamber in the normal aging human eye. *Arch Ophthalmol.* 1980;98(10):1803–1808.
93. Heichel J, Wilhelm F, Kunert KS, Hammer T. Topographic findings of the porcine cornea. *Med Hypothesis Discov Innov Ophthalmol.* 2016;5:125–131.
94. Yang J, Wang X, Fuh G, et al. Comparison of binding characteristics and in vitro activities of three inhibitors of vascular endothelial growth factor A. *Mol Pharm.* 2014;11(10):3421–3430.
95. Eden E, Geva-Zatorsky N, Issaeva I, et al. Proteome half-life dynamics in living human cells. *Science.* 2011;331(6018):764–768.
96. Dörrbaum AR, Kochen L, Langer JD, Schuman EM. Local and global influences on protein turnover in neurons and glia. *eLife.* 2018;7:e34202.

Investigative Ophthalmology & Visual Science

Downloaded from iovs.arvojournals.org on 09/24/2025

97. Jakubowski H, Flatt P, eds, *Fundamentals of Biochemistry*. LibreTexts; 2024, https://bio.libretexts.org/@go/page/14985.
98. Gadkar K, Pastuskovas CV, Le Couter JE, et al. Design and pharmacokinetic characterization of novel antibody formats for ocular therapeutics. *Invest Ophthalmol Vis Sci.* 2015;56(9):5390–5400.
99. Muether PS, Hermann MM, Viebahn U, Kirchhof B, Fauser S. Vascular endothelial growth factor in patients with exudative age-related macular degeneration treated with ranibizumab. *Ophthalmology*. 2012;119(10):2082–2086.
100. Saunders DJ, Muether PS, Fauser S. A model of the ocular pharmacokinetics involved in the therapy of neovascular age-related macular degeneration with ranibizumab. *Br J Ophthalmol.* 2015;99(11):1554–1559.
101. Dartt DA, Willcox MDP. Complexity of the tear film: importance in homeostasis and dysfunction during disease. *Exp Eye Res.* 2013;117:1–3.
102. Sørensen T, Jensen FT. Tear flow in normal human eyes. determination by means of radioisotope and gamma camera. *Acta Ophthalmol.* 1979;57(4):564–581.
103. Wakabayashi Y, Usui Y, Okunuki Y, et al. Intraocular VEGF level as a risk factor for postoperative complications after vitrectomy for proliferative diabetic retinopathy. *Invest Ophthalmol Vis Sci.* 2012;53(10):6403–6410.
104. Li B, Li M-D, Ye J-J, Chen Z, Guo Z-J, Di Y. Vascular endothelial growth factor concentration in vitreous humor of patients with severe proliferative diabetic retinopathy after intravitreal injection of conbercept as an adjunctive therapy for vitrectomy. *Chin Med J.* 2020;133(6):664–669.
105. Muhiddin HS, Kamaruddin MI, Ichsan AM, Budu. Vitreous and serum concentrations of vascular endothelial growth factor and platelet-derived growth factor in proliferative diabetic retinopathy. *Clin Ophthalmol.* 2020;14:1547–1552.
106. Shimada H, Akaza E, Yuzawa M, Kawashima M. Concentration gradient of vascular endothelial growth factor in the vitreous of eyes with diabetic macular edema. *Invest Ophthalmol Vis Sci.* 2009;50(6):2953–2955.
107. Wang J, Chen S, Jiang F, et al. Vitreous and plasma VEGF levels as predictive factors in the progression of proliferative diabetic retinopathy after vitrectomy. *PLoS One.* 2014;9(10):1–8.
108. Wells JA, Murthy R, Chibber R, et al. Levels of vascular endothelial growth factor are elevated in the vitreous of patients with subretinal neovascularisation. *Br J Ophthalmol.* 1996;80(4):363–366.

Appendix: Parameter Justification

- **Time for tear volume to return to normal (human)/time for eye drop to leave cornea (porcine), τ_{loss}**
  - In vivo human eye: estimates of the time taken for the tear volume to return to normal following the application of a drop range 1–5 min = 1.67–8.33 × 10^{-2} h.[39–43] We assume that τ_{loss} could lie anywhere within this range, taking the mean value of 3 min = 5 × 10^{-2} h as our default.
  - Ex vivo porcine eye: it is difficult to characterize the time taken for a drop to flow off of the cornea; however, observations during our experiments suggest that the majority of the drop volume remains on the cornea during the experiment (the constant volume scenario). When considering the depleting volume scenario, we assume that the time scale is similar to that for the human tear volume to return to normal, given above. Therefore, we take a value of 3 min = 5 × 10^{-2} h as our default, with a possible range of 1.67–8.33 × 10^{-2} h.
- **Volume of eye drop (human and porcine), V_{Drop}:** the volume of the eye drop used in our experiments is 4.5 × 10^{-2} mL and we assume the same volume for human treatment. For the sensitivity analysis, we assume that V_{Drop} could vary over a range 10% above and below its default value, giving the range 4.05–4.95 × 10^{-2} mL.
- **Volume of normal tear film (human), $V_{\text{Tear}_{\text{Norm}}}$:** the normal volume of the human tear film has been measured to range 3.4–10.7 × 10^{-3} mL.[44,45] We assume that $V_{\text{Tear}_{\text{Norm}}}$ could lie anywhere within this range, taking the mean of the mean values stated in Mishima et al.[44] and Scherz et al.,[45] that is 6.35 × 10^{-3} mL, as our default value (see also other sources[39,40,42,46,47,89–91]).
- **Volume of tear reservoir (human), $V_{\text{Tear}_{\text{Res}}}$:** the human tear reservoir volume has been measured to be 3 × 10^{-2} mL.[40,42,46,47] For the sensitivity analysis, we assume that $V_{\text{Tear}_{\text{Res}}}$ could vary over a range 10% above and below its default value, giving the range 2.70–3.30 × 10^{-2} mL.
- **Volume of aqueous, V_{Aq}**
  - In vivo human eye: the volume of the aqueous in the healthy human eye decreases with age, with values of 0.247 ± 0.039 mL in people aged 20–30 years and values of 0.160 ± 0.039 mL in people aged 60 years and older.[48] We take a value of 0.160 mL as our default, since patients being treated for wet AMD will typically be 60 years and older, and assume that V_{Aq} could lie anywhere in the range 0.121–0.286 mL (where 0.121 = 0.160 − 0.039 and 0.286 = 0.247 + 0.039; see also other sources[17,92]).
  - Ex vivo porcine eye: the aqueous volume of the pig eye has been measured to be 0.31 mL.[49,50]
- **Volume of vitreous, V_{Vit}**
  - In vivo human eye: the volume of the vitreous has been measured to lie in the range 3.5–5.4 mL,[49] with quoted volumes of 4 mL[54] and 4.5 mL[17,51,52] being common. We assume that V_{Vit} could lie anywhere within the range 3.5–5.4 mL, taking a value of 4.5 mL as our default since it lies in the middle of this range and is a frequently quoted value.
  - Ex vivo porcine eye: the vitreal volume of the pig eye has been measured to lie in the range 3.0–3.2 mL.[49,50,53,54,] We assume that

Investigative Ophthalmology & Visual Science

Downloaded from iovs.arvojournals.org on 09/24/2025

V_{Vit} could lie anywhere within this range, taking the middle value of 3.1 mL as our default.

- **Area of the tear-aqueous interface, $A_{Tear\text{-}Aq}$**
  - In vivo human eye: Rüfer et al.[56] measured the corneal diameter of human eyes to range across 1.07–1.26 cm, with an average diameter of 1.17 cm, while Bron et al.[55] quote a horizontal diameter of 1.175 cm and a vertical diameter of 1.06 cm. Bron et al.[55] also give the corneal anterior radius of curvature as 0.78 cm. Approximating the cornea as a flat disc, Rüfer et al.'s measurements correspond to corneal areas in the range 0.899–1.24 cm^2 with a mean value of 1.08 cm^2, while approximating the cornea as a flat ellipse, Bron et al.'s measurements correspond to an area of 0.978 cm^2. If we instead use a surface integral to calculate the corneal anterior area, using the corneal anterior radius of curvature, then Rüfer et al.'s measurements correspond to areas ranging across 1.04–1.56 cm^2 with a mean value of 1.30 cm^2, while Bron et al.'s measurements correspond to an area of 1.16 cm^2. The corneal area quoted by Bron et al.[55] is 1.06 cm^2. This is smaller than our calculated area based on Bron et al.'s diameters, but within the range of areas calculated from Rüfer et al.'s diameters. We assume that corneal area may range across 1.04–1.56 cm^2 and take 1.30 cm^2 as our default value.
  - Ex vivo porcine eye: the corneal surface area of "large" porcine eyes has been measured to be 1.40 ± 0.19 cm^2.[57] We scale this value for eyes of the dimensions used in our experiments as follows. The mean scleral surface area of the "large" porcine eyes noted above was measured to be 11.92 cm^2,[57] giving a total mean surface area of 13.32 cm^2 (assuming that the limbal surface area is included in the scleral surface area). Thus, the proportion of the eye surface area taken up by the cornea is 0.105 (this proportion would appear to be scale-invariant, given that it is maintained for their measurements of "small"- and "medium"-sized pig eyes—these being 0.123 and 0.106, respectively). We measured the length and width of each of the eyes used in our experiments (providing similar values to those given in previous studies[49,64]). Taking the average of these two diameters for each eye and approximating the eye's geometry as a sphere, we calculated each eye's surface area. This gave a mean total surface area across all eyes of 14.40 cm^2, with a range of 12.33–16.74 cm^2. Assuming that the proportion of the eye's surface area taken up by the cornea is the same as in Olsen et al.,[57] we take the default corneal surface area to be 1.51 cm^2, with a possible range of 1.30–1.76 cm^2. This is also within the range of values that can be extrapolated from measurements in Heichel et al.[93] and Sanchez et al.[63]
- **Area of the aqueous-vitreous interface, $A_{Aq\text{-}Vit}$**
  - In vivo human eye: the aqueous-vitreous interface consists of the suspensory ligaments that span an annular region between the ciliary body and the lens (holding it in place). We calculate its area as follows. Manns et al.[58] measured the lens diameter and inner ciliary body diameter in three groups of individuals: a young group (8–19 years), an older group of prepresbyopic donors (20–70 years), and an older group of presbyopic donors (20–70 years). The mean lens diameter across all three groups was 0.90 cm and ranged from 0.84–0.97 cm, while the mean inner ciliary body diameter across all three groups was 1.12 cm and ranged from 1.04–1.17 cm. This corresponds to lens areas ranging from 0.554–0.739 cm^2, with a mean of 0.636 cm^2, and areas spanned by the inner ciliary body ranging from 0.849–1.08 cm^2, with a mean of 0.985 cm^2. Thus, the mean aqueous-vitreous interface area ranges from 0.111–0.521 cm^2 (taking this as our sensitivity analysis range), with a mean (default) value of 0.349 cm^2 (which is also the mean area of the older prepresbyopic group).
  - Ex vivo porcine eye: in the absence of an inner ciliary body diameter measurement, we calculate its area as follows. The scleral outer radius is 1.112 cm[64] (calculated to match the area value in Olsen et al.[57]). The combined width of the retina and choroid varies across the eye, with a range of 0.02–0.086 cm,[55,63,64] while the scleral width is 0.043–0.089 cm.[57,64] Subtracting the mean values of the retina-choroid and scleral widths from the scleral outer radius gives us the radius of the vitreous as 0.993 cm. (We note that this is consistent with the vitreal volume stated above, which, assuming a spherical vitreous, corresponds to a radius of 0.905 cm.) The length of the eye (in the transverse/sagittal planes) is 2.29 cm,[64] the corneal width is 0.098 cm at its apex,[59,64] and the anterior segment depth (that is, the lens equator position, posterior to the posterior surface of the cornea) is 0.247 cm.[60,62,64] Subtracting the scleral outer radius, the apex corneal width, and the anterior segment

Investigative Ophthalmology & Visual Science

Downloaded from iovs.arvojournals.org on 09/24/2025

depth from the length of the eye gives us the distance between the center of the vitreous and the lens equator as 0.833 cm. Using the Pythagorean theorem, this gives the radius of the aqueous-vitreous interface, including the lens, as $\sqrt{0.993^2 - 0.833^2} = 0.541$ cm. Therefore, the area of the aqueous-vitreous interface, including the lens, is 0.918 cm^2. The lens has (unstretched) diameter of 0.886 cm[61] and hence an area of 0.617 cm^2. Therefore, the area of the aqueous-vitreous interface, not including the lens, is $0.918 - 0.617 = 0.301$ cm^2.

- **Area of the vitreo-retinal interface (human), $A_{\text{Vit-Ret}}$:** this has been calculated to be 10.9 cm^2 (our default value)[65] and is similar to the value given for the choroidal surface area of 11.8 cm^2 by Bron et al.[55] For the sensitivity analysis, we assume that $A_{\text{Vit-Ret}}$ could vary over a range 10% above and below its default value, giving the range 9.81–12.0 cm^2.
- **Binding rate of R to VR (to form RVR—human and porcine), k^+:** Papadopoulos et al.[66] have measured a binding rate of ranibizumab to VEGF of 1.60×10^5 M^{-1} s^{-1}, converting to units consistent with our model, which is 0.576 $pmol^{-1}$ mL h^{-1} (our default value). This is within the range of values measured by Yang et al.,[94] 0.205–4.21 $pmol^{-1}$ mL h^{-1} (following conversion, which we take as our range), and similar to the default value used by Hutton-Smith et al.[17]
- **Unbinding rate of VR (to form V + R—human and porcine), k^-:** Papadopoulos et al.[66] have measured an unbinding rate of ranibizumab from VEGF of 7.30×10^{-6} s^{-1}, converting to units consistent with our model, which is 2.63×10^{-2} h^{-1} (our default value). This is within the range of values measured by Yang et al.,[94] $1.40–3.60 \times 10^{-2}$ h^{-1} (following conversion, which we take as our range), and similar to the default value used by Hutton-Smith et al.[17] The default values of k^+ and k^- give us an equilibrium dissociation constant, $K_D = \frac{k^-}{k^+} = 4.56 \times 10^{-2}$ pmol mL^{-1}. This is the same value used by Hutton-Smith et al.[17] and within the range of values resulting from Yang et al.'s[94] measurements.
- **Rate of molecular degradation, $\delta_{i,j}$ (for $i \in$ {Aq, Vit} and $j \in \{v, r, u, w\}$—human and porcine):** as a simplifying assumption, we neglect molecular degradation by default, assuming that it is negligible compared to the speed of the other processes captured in our model in the in vivo human eye and absent in the ex vivo porcine eye (indeed, molecular degradation is not typically included in models of anti-VEFG treatments; see, for example, other sources[17–19]). Eden et al.[95] measured protein half-lives in the range 0.9–20.5 h in living human cells, while Dörrbaum et al.[96] measured the majority of protein half-lives to lie in the range 1–20 days in rat primary hippocampal, neuron-enriched, and glia-enriched cultures. Combining the results of these two studies gives us decay rates in the range 1.44×10^{-3} –0.770 h^{-1}. Thus, we assume that the decay rates could lie anywhere in the range 0–0.770 h^{-1} in the in vivo human eye.
- **Permeability of the tear-aqueous interface to R with CPP, $\beta_{\text{Tear-Aq},r}$, and permeability of the aqueous-vitreous interface to R, $\beta_{\text{Aq-Vit},r}$**
  - Ex vivo porcine eye: these parameters are determined by fitting the porcine version of our mathematical model to our experimental data. We note that these are the only two parameters to be obtained by fitting to experimental data, the permeability of the aqueous-vitreous interface to V/VR/RVR being inferred from its permeability to R and the equivalent human permeability values being inferred from the porcine values (see below), while all other parameters are determined from the literature or directly from our experimental data (or from the model steady-state in the case of $v_{\text{Aq}_{\text{init}}}$ and $v_{\text{Vit}_{\text{init}}}$—see below). In the fitted model, we neglect VEGF (V) and both of its compounds with ranibizumab (VR and RVR), since the measured concentration of ranibizumab in the aqueous and vitreous reaches at least 0.1 pmol mL^{-1} for topical application and almost 5 pmol mL^{-1} for intravitreal administration, while the measured concentration of VEGF never exceeds 3×10^{-2} pmol mL^{-1} and is almost always 1×10^{-2} pmol mL^{-1} or below (one to two orders of magnitude smaller than the ranibizumab concentrations). Thus, we are only solving (governing) Equations 3, 5, 9 and 13 for the topical treatment case and Equations 5 and 9 for the intravitreal treatment case. We performed two main fittings. First, for the topically applied treatment, we fit for $\beta_{\text{Tear-Aq},r}$ and $\beta_{\text{Aq-Vit},r}$ to the mean aqueous ranibizumab data points at 20 min, 40 min, and 3.5 h, neglecting the 1-h data point since we lack confidence in the measurements at that time point (at which no ranibizumab was detected—see the Experimental Results section), and neglecting the vitreal ranibizumab measurements since they take values within the range of the

Investigative Ophthalmology & Visual Science

Downloaded from iovs.arvojournals.org on 09/24/2025

control measurements in the vitreous and are inconsistent with the measured values in the aqueous, given that vitreal concentrations should be lower than those in the aqueous for a concentration gradient to be established, where in fact they are measured to be higher (see the Experimental Results section). This gives $\beta_{\text{Tear-Aq},r} = 5.93 \times 10^{-7}$ cm h^{-1} and $\beta_{\text{Aq-Vit},r} = 0.929$ cm h^{-1}. In the second fitting, for intravitreal treatment without CPP, we fit for $\beta_{\text{Aq-Vit},r}$, taking the mean aqueous and vitreal ranibizumab data points at 20 min as our initial conditions and fitting to the mean aqueous ranibizumab data points at 40 min, 1 h, and 3.5 h. We take the data points at 20 min as our initial conditions (rather than the calculated vitreal and aqueous concentrations at $t = 0$ h) since the measured vitreal ranibizumab concentration is smaller than we would expect, based on the dose administered to the vitreous (see the Experimental Results section). We do not fit to the ranibizumab data points in the vitreous since these are uninformative, being essentially constant over time. This gives $\beta_{\text{Aq-Vit},r} = 0.577$ cm h^{-1}. The topical fit provides a good fit in both cases and actually does a better job in fitting to the $t = 3.5$ h data point in the aqueous for intravitreal treatment than the second model fit. Therefore, we consider the topical model fit to be preferable, taking this as our default for the ex vivo porcine eye (see the Model Fitting section for further details).

  - In vivo human eye: we infer the human values from the porcine values, noting that the permeability of a barrier to a chemical is $\beta = D/\Delta x$ (cm h^{-1}),[97] where D (cm^2 h^{-1}) is the diffusivity of the chemical species within the barrier and Δx (cm) is the width of the barrier. We assume that the diffusivity of ranibizumab within the cornea and suspensory ligaments is the same in porcine and human eyes. The porcine cornea has a mean width (anterior-posterior surface) of about 9.6×10^{-2} cm,[59,64] while the human corneal width is about 5.2×10^{-2} cm.[24,55] Scaling accordingly, this gives a default human corneal permeability to ranibizumab of $\beta_{\text{Tear-Aq},r} = (9.6/5.2) \times 5.93 \times 10^{-7} = 1.10 \times 10^{-6}$ cm h^{-1}. The suspensory ligaments (or zonule) have a width (anterior-posterior) of up to 0.255 cm in humans.[55] We were unable to find an equivalent measurement for the porcine eye. Given that porcine and human eye dimensions are similar, we assume the zonule width is the same. Therefore, the human default value for $\beta_{\text{Aq-Vit},r}$ is assumed to be the same as for the pig, which is 0.929 cm h^{-1}. For the sensitivity analysis, we assume that $\beta_{\text{Tear-Aq},r}$ and $\beta_{\text{Aq-Vit},r}$ could vary over a range 10% above and below their default values, giving the ranges 0.990–1.21×10^{-6} cm h^{-1} and 0.836–1.02 cm h^{-1}, respectively.

- **Permeability of the aqueous-vitreous interface to V/VR/RVR (human and porcine), $\beta_{\text{Aq-Vit},j}$ (for $j \in \{v, u, w\}$):** we infer the permeability of the suspensory ligaments (or zonule) to VEGF and its compounds with ranibizumab (V, VR, and RVR) from the fitted permeability for ranibizumab (R, see above), assuming, as for $\beta_{\text{Aq-Vit},r}$, that the permeabilities do not differ between the human and porcine eye. As noted above, the permeability of a barrier to a given chemical species is directly proportional to the diffusivity of that species ($\beta = D/\Delta x$).[97] Hutton-Smith et al.[17] calculated the diffusivities of V, R, VR, and RVR using the Stokes–Einstein relation (at 37°C in physiological saline) and the molecular weights of R and V as found in Ferrara et al.[67] and Penn et al.,[68] respectively (inferring the molecular weights of VR and RVR by adding the weights of R and V). This gave the diffusivities of V, R, VR, and RVR as $D_v = 5.11 \times 10^{-3}$ cm^2 h^{-1}, $D_r = 4.82 \times 10^{-3}$ cm^2 h^{-1}, $D_u = 3.92 \times 10^{-3}$ cm^2 h^{-1}, and $D_w = 3.39 \times 10^{-3}$ cm^2 h^{-1}, respectively. Thus, $\beta_{\text{Aq-Vit},v} = (D_v/D_r)\beta_{\text{Aq-Vit},r} = 0.985$ cm h^{-1}, $\beta_{\text{Aq-Vit},u} = (D_u/D_r)\beta_{\text{Aq-Vit},r} = 0.755$ cm h^{-1}, and $\beta_{\text{Aq-Vit},w} = (D_w/D_r)\beta_{\text{Aq-Vit},r} = 0.653$ cm h^{-1}. For the sensitivity analysis, we assume that $\beta_{\text{Aq-Vit},v}$, $\beta_{\text{Aq-Vit},u}$, and $\beta_{\text{Aq-Vit},w}$ could vary over a range 10% above and below their default values, giving the ranges 0.887–1.08 cm h^{-1}, 0.680–0.831 cm h^{-1}, and 0.588–0.718 cm h^{-1}, respectively.
- **Permeability of the vitreo-retinal interface to R/VR/RVR, $\beta_{\text{Vit-Ret},j}$ (for $j \in \{r, u, w\}$):**
  - In vivo human eye: permeabilities of the inner limiting membrane to R, RV, and RVR were calculated by Hutton-Smith et al.[19] using equations relating a species' retinal permeability to its hydrodynamic radius derived in Hutton-Smith et al.,[18] which utilized data from Gadkar et al.[98] Values were calculated as $\beta_{\text{Vit-Ret},r} = 6.80 \times 10^{-4}$ cm h^{-1}, $\beta_{\text{Vit-Ret},u} = 6.44 \times 10^{-4}$ cm h^{-1}, and $\beta_{\text{Vit-Ret},w} = 6.23 \times 10^{-4}$ cm h^{-1}. For the sensitivity analysis, we assume that $\beta_{\text{Vit-Ret},r}$, $\beta_{\text{Vit-Ret},u}$, and $\beta_{\text{Vit-Ret},w}$ could vary over a range 10% above and below their default values, giving the ranges $6.12–7.48 \times 10^{-4}$ cm h^{-1}, 5.80–

Downloaded from iovs.arvojournals.org on 09/24/2025

7.08 × 10^{-4} cm h^{-1}, and 5.61–6.85 × 10^{-4} cm h^{-1}, respectively.
  - Ex vivo porcine eye: we set $\beta_{\text{Vit-Ret},r} = 0$ cm h^{-1}, $\beta_{\text{Vit-Ret},u} = 0$ cm h^{-1}, and $\beta_{\text{Vit-Ret},w} = 0$ cm h^{-1} since there is no choroidal blood flow in the ex vivo porcine eye, and hence a concentration gradient will not be maintained to sustain a net flux of ranibizumab and its compounds into the retina. Further, the volume of the retina is over an order of magnitude smaller than that of the vitreous;[19] thus, the effect of the flux of ranibizumab and its compounds into the retina is negligible.
- **Rate at which retina contributes V to vitreous, $\phi_{\text{Vit},v}$**
  - In vivo human eye: Hutton-Smith et al.[17] fitted their two-compartment (aqueous and vitreous) model to individual patients across Muether and Saunders et al.'s[79,99,100] human data. We take their mean fitted value, $\phi_{\text{Vit},v} = 2.34 \times 10^{-4}$ pmol h^{-1}, as our default, and take the minimum and maximum fitted values, 1.02 × 10^{-4} and 4.46 × 10^{-4} pmol h^{-1}, as our range for sensitivity analysis. We note that in a later paper, Hutton-Smith et al.[19] refit this parameter for a three-compartment model (aqueous, vitreous, and retina), such that it contributes VEGF to the retina, rather than directly to the vitreous, obtaining a mean value of 7.29 × 10^{-4} pmol h^{-1} and a range of 2.50 × 10^{-4} to 1.58 × 10^{-3} pmol h^{-1}. These values are similar to, though larger than, the earlier fitted values. We consider the earlier values to be more relevant for our model, since both our model and that of Hutton-Smith et al.[17] neglect the retinal compartment and since the additional VEGF produced in the three-compartment model is lost to the choroid, rather than contributing to the vitreal supply of VEGF.
  - Ex vivo porcine eye: we set $\phi_{\text{Vit},v} = 0$ pmol h^{-1} since there is no VEGF production in an ex vivo eye.
- **Rate of inflow/outflow to/from tear film, ψ_{Tear}**
  - In vivo human eye: the turnover rate of tear fluid in the human eye has been measured to range from 3.0–13.2 × 10^{-2} mL h^{-1}, with a mean value of 7.2 × 10^{-2} mL h^{-1}[44] (see also other sources[39,42,45,47,89,91,101,102]). We do not include evaporative tear loss since the rate of evaporation (approx. 6 × 10^{-3}mL h^{-1})[102] is an order of magnitude smaller than the total rate of tear turnover, and since ranibizumab is nonvolatile and hence will not be lost through evaporation (with ranibizumab-free fluid lost through evaporation being replaced by ranibizumab-free serous fluid produced by the lacrimal gland).
  - Ex vivo porcine eye: since there is no tear fluid production in the ex vivo porcine eye, there is no dilution effect, and hence $\psi_{\text{Tear}} = 0$ mL h^{-1}. As in humans, we neglect evaporative tear loss, noting that visual observation suggests that the majority of the drop remains on the cornea during the course of the experiment.
- **Rate of inflow/outflow to/from aqueous, ψ_{Aq}**
  - In vivo human eye: we take $\psi_{\text{Aq}} = 0.15$ mL h^{-1} with Hutton-Smith et al.[17,19] and Missel.[24] Hutton-Smith et al.[17] take their value from Tasman and Jaeger,[70] who cite values in the range 0.12–0.15 mL h^{-1} (across seven studies), while Missel[24] takes the mean value from eight studies in normal humans summarized in Table 1 of McLaren,[69] which contains values ranging from 6.6 × 10^{-2}–0.25 mL h^{-1}. We take this latter interval as our range for sensitivity analysis.
  - Ex vivo porcine eye: since there is no aqueous production (or drainage) in the ex vivo porcine eye, there is no dilution effect, and hence $\psi_{\text{Aq}} = 0$ mL h^{-1}.
- **Initial V concentration in aqueous, $v_{\text{Aq}_{\text{init}}}$**
  - In vivo human eye: we set the initial VEGF concentration equal to its modeled equilibrium value in the absence of ranibizumab, giving a default value of $v_{\text{Aq}_{\text{init}}} = 1.56 \times 10^{-3}$ pmol mL^{-1}. Comparing with values in the literature, Saunders et al.[100] measured VEGF concentrations in patients with AMD to lie in the range 7.5 × 10^{-4}–2.8 × 10^{-3} pmol mL^{-1} with a mean value of 1.6 × 10^{-3} pmol mL^{-1}, while Wakabayashi et al.[103] measured VEGF values in the range 1.13 × 10^{-4}–2.82 × 10^{-2} pmol mL^{-1} with a mean value of 2.78 × 10^{-3} pmol mL^{-1} in patients with proliferative diabetic retinopathy (and without early vitreous hemorrhage), and Hutton-Smith et al.[17,19] derive values of ∼1.7 × 10^{-3} or ∼1.75 × 10^{-3} pmol mL^{-1} as the equilibrium solution to the ranibizumab-free problem. These values are all similar, with the measurements from Saunders et al.[100] being the most relevant to the present study since they are from patients with AMD. We note that our simulated value is equal to Saunders et al.'s mean value to an accuracy of two significant figures.
  - Ex vivo porcine eye: as noted in the $\beta_{\text{Tear-Aq},r}$ and $\beta_{\text{Aq-Vit},r}$ parameter justification section above, we neglect VEGF in porcine simulations.

Investigative Ophthalmology & Visual Science

Downloaded from iovs.arvojournals.org on 09/24/2025

- **Initial V concentration in vitreous, $v_{\text{Vit}_{\text{init}}}$**
  - In vivo human eye: we set the initial VEGF concentration equal to its modeled equilibrium value in the absence of ranibizumab, giving a default value of $v_{\text{Vit}_{\text{init}}} = 2.24 \times 10^{-3}$ pmol mL^{-1}. Comparing with values in the literature, we note that measured values in humans vary widely, with reported mean values ranging from 5×10^{-6}–9.44×10^{-1} pmol mL^{-1} (across healthy individuals and patients with proliferative diabetic retinopathy, subfoveal neovascular membrane, idiopathic full-thickness macular hole, and AMD),[52,103–108] with reported values for patients with AMD ranging from 5×10^{-6}–8.48×10^{-4} pmol mL^{-1}.[52] We note that our simulated value is within the range of measured values in humans and just above the single measured range in patients with AMD.
  - Ex vivo porcine eye: as noted in the $\beta_{\text{Tear-Aq},r}$ and $\beta_{\text{Aq-Vit},r}$ parameter justification section above, we neglect VEGF in porcine simulations.
- **R dose concentration, r_{Dose}:** the ranibizumab concentration in both the eye drop and the intravitreal injection is 1 mg mL^{-1} = 10^9 pg mL^{-1}. For our model, we require units of pmol mL^{-1}. We can convert to these units by dividing the ranibizumab concentration in pg mL^{-1} by its molecular weight/molar mass,[17,67] which is 48.35 kDa = 48,350 g mol^{-1} = 48,350 pg pmol^{-1} to give 2.07×10^4 pmol mL^{-1}. For the sensitivity analysis, we assume that r_{Dose} could vary over a range 10% above and below its default value, giving the range 1.86–2.28×10^4 pmol mL^{-1}.
- **Initial R concentration in tear, $r_{\text{Tear}_{\text{init}}}$**
  - In vivo human eye: when a drop is applied (with volume V_{Drop}), its contents will rapidly merge with the existing tear film (with volume $V_{\text{Tear}_{\text{Norm}}}$) before the excess fluid flows off of the cornea. Assuming that this is the first drop to be applied, the ranibizumab concentration will therefore be $r_{\text{Dose}} \frac{V_{\text{Drop}}}{V_{\text{Drop}}+V_{\text{Tear}_{\text{Norm}}}} = 1.81 \times 10^4$ pmol mL^{-1}, assuming the default value of $V_{\text{Tear}_{\text{Norm}}}$ (see discussion of $V_{\text{Tear}_{\text{Norm}}}$ above).
  - Ex vivo porcine eye: in this case, there is no tear film to dilute the dose since the only fluid on the surface of the cornea is from the drop; therefore, $r_{\text{Tear}_{\text{init}}} = r_{\text{Dose}} = 2.07 \times 10^4$ pmol mL^{-1}.
- **Initial R concentration in vitreous, $r_{\text{Vit}_{\text{init}}}$**
  - In vivo human eye: when an intravitreal injection is administered (with volume V_{Drop}), it is assumed that the ranibizumab concentration quickly equilibrates throughout the vitreous (with volume V_{Vit}, given the mixing effect of saccadic eye rotations[21–23,25,26]), such that $r_{\text{Vit}_{\text{init}}} = \frac{r_{\text{Dose}} V_{\text{Drop}}}{V_{\text{Vit}}}$. It is assumed that the injected volume does not affect the vitreal volume, with the additional volume being negligible (given that $V_{\text{Drop}} \ll V_{\text{Vit}}$) and quickly drained. Therefore, $r_{\text{Vit}_{\text{init}}} = 2.07 \times 10^2$ pmol mL^{-1}, assuming the default value of V_{Vit} (see discussion of V_{Vit} above).
  - Ex vivo porcine eye: we use the mean measured value at $t = 20$ min from our experiments for intravitreal ranibizumab injection without CPP, giving a value of $r_{\text{Vit}_{\text{init}}} = 4.29$ pmol mL^{-1}. Were we to have calculated this parameter in the same way as for the in vivo human eye, this would have given a value of $r_{\text{Vit}_{\text{init}}} = 3.00 \times 10^2$ pmol mL^{-1} (see the Experimental Results and Model Fitting sections for a discussion).

Investigative Ophthalmology & Visual Science

Downloaded from iovs.arvojournals.org on 09/24/2025